

## Lehigh University Lehigh Preserve

---

### Theses and Dissertations

---

1-1-1978

# Static and dynamic fracture behavior of A737 Grade B steel.

Javaid Iqbal Qureshi

Follow this and additional works at: <http://preserve.lehigh.edu/etd>

 Part of the [Materials Science and Engineering Commons](#)

---

### Recommended Citation

Qureshi, Javaid Iqbal, "Static and dynamic fracture behavior of A737 Grade B steel." (1978). *Theses and Dissertations*. Paper 2055.

This Thesis is brought to you for free and open access by Lehigh Preserve. It has been accepted for inclusion in Theses and Dissertations by an authorized administrator of Lehigh Preserve. For more information, please contact [preserve@lehigh.edu](mailto:preserve@lehigh.edu).

STATIC AND DYNAMIC FRACTURE  
BEHAVIOR OF A737 GRADE B STEEL

JAVAID IQBAL QURESHI

A Thesis

Presented to the Graduate Committee

of Lehigh University

in Candidacy for the Degree of

Master of Science

in

Metallurgy and Materials Engineering

Lehigh University

1978

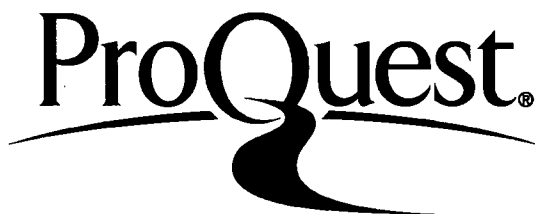
ProQuest Number: EP76328

All rights reserved

INFORMATION TO ALL USERS

The quality of this reproduction is dependent upon the quality of the copy submitted.

In the unlikely event that the author did not send a complete manuscript and there are missing pages, these will be noted. Also, if material had to be removed, a note will indicate the deletion.



ProQuest EP76328

Published by ProQuest LLC (2015). Copyright of the Dissertation is held by the Author.

All rights reserved.

This work is protected against unauthorized copying under Title 17, United States Code  
Microform Edition © ProQuest LLC.

ProQuest LLC.  
789 East Eisenhower Parkway  
P.O. Box 1346  
Ann Arbor, MI 48106 - 1346

This thesis is accepted in partial fulfillment of  
the requirements for the degree of Master of Science.

11 October  
(Date)

\_\_\_\_\_  
Professor in Charge

\_\_\_\_\_  
Chairman, Department of  
Metallurgy & Materials Eng'g.

## ACKNOWLEDGEMENTS

I express my sincere thanks to all persons who made this work possible, especially to my thesis advisor, Dr. Alan W. Pense for his sincere guidance during this investigation. Their efforts are great and my gratitude is profound. I also appreciate the patience of my wife during the completion of this work.

I am deeply indebted to Pressure Vessel Research Committee for their generous financial support and Lukens Steel for supplying material.

## TABLE OF CONTENTS

ABSTRACT	1
INTRODUCTION	2
TEST MATERIALS	8
TESTING PROCEDURES	9
Tension and Charpy Impact Tests	9
Fracture Toughness Tests	9
Metallographic Examination	14
RESULTS AND DISCUSSION	15
Tension and Impact Tests	15
Metallography	16
Static Fracture Toughness	17
Dynamic Fracture Toughness	20
Fracture Toughness Summary	21
CONCLUSIONS	23
TABLES	25 - 32
FIGURES	33 - 56
REFERENCES	57
VITA	

## LIST OF TABLES

Table	Title
1	Chemistry and Mechanical Property Data for A737B Steel - Normal Sulfur
2	Chemistry and Mechanical Property Data for A737B Steel - Low Sulfur
3	Tension Test Data for A737B Steel
4	Static Fracture Toughness Results for A737 Grade B Normal Sulfur Heats - Transverse
5	Static Fracture Toughness Data for A737 Grade B Low Sulfur Heat - Transverse
6	Dynamic Fracture Toughness Data for A737 Grade B Normal Sulfur Heats - Transverse
7	Dynamic Fracture Toughness Data for A737 Grade B Low Sulfur Heats - Transverse
8	Summary of Fracture Toughness Data for A737 Grade B Transverse Properties

## LIST OF FIGURES

Figure	Title
1	2-inch Thickness Compact Specimen
2	Time vs Load Trace of Dynamic Loading
3	Graphic Representation of Yield Strength vs Temperature of Low and Normal Sulfur A737-B Steel
4	Tensile Strength vs Temperature of Low and Normal Sulfur A737-B Steel
5	Elongation vs Temperature of Low and Normal Sulfur of A737-B Steel
6	Charpy Energy Absorbed vs Temperature of Quarter and Center Thickness of Normal Sulfur Normalized A737-B Steel
7	Charpy Energy Absorbed vs Temperature of Quarter and Center Thickness of Normal Sulfur Quenched and Tempered A737-B Steel
8	Charpy Energy Absorbed vs Temperature at Quarter and Center Thickness of Low Sulfur Quenched and Tempered A737-B Steel
9	Charpy Energy Absorbed vs Temperature at Quarter and Center Thickness of Low Sulfur Normalized A737-B Steel
10	Microstructure of the Normal Sulfur A737-B Steel
11	Microstructure of the Low Sulfur A737-B Steel
12	J vs $\Delta a$ Curves for Normal Sulfur Normalized A737-B Steel at 23°C.



- 13 J vs  $\Delta a$  Curve for Normal Sulfur Quenched and Tempered A737-B Steel at 23°C
- 14 J vs  $\Delta a$  Curve for Normal Sulfur Quenched and Tempered A737-B Steel at -41°C
- 15 J vs  $\Delta a$  Curve for Low Sulfur Normalized A737-B Steel at 23°C
- 16 J vs  $\Delta a$  Curve for Low Sulfur Quenched and Tempered A737-B Steel at 23°C
- 17 J vs  $\Delta a$  Curve for Low Sulfur Normalized A737-B Steel at -46°C
- 18 J vs  $\Delta a$  Curve for Low Sulfur Quenched and Tempered A737-B Steel at -46°C
- 19 Temperature Dependence of Static Fracture Toughness of Low and Normal Sulfur in Normalized and Quenched & tempered A737-B Steel
- 20 Temperature Dependence of Dynamic Fracture Toughness of Low and Normal Sulfur in Normalized and Quenched & Tempered A737-B Steel
- 21 Temperature vs Static and Dynamic Fracture Toughness of Normal Sulfur in Normalized and Quenched & Tempered
- 22 Temperature vs Static and Dynamic Fracture Toughness of Low Sulfur in Normalized and Quenched & Tempered A737-B Steel
- 23 Temperature vs Fracture Performance of  $\left(\frac{K_{Ic}}{\sigma_y}\right)$  of Normal Sulfur in Normalized and Quenched and Tempered A737-A Steel

24 Temperature vs Fracture Performance ( $\frac{K_{Ic}}{\sigma_y}$ ) of Low  
Sulfur in Normalized and Quenched and Tempered  
A737-B Steel

## ABSTRACT

An experimental program was conducted on the strength and toughness of A737 Grade B carbon-manganese-columbium pressure vessel steel in two conditions of heat treatment and at two levels of sulfur content. The steel was tested in the normalized and in the quenched and tempered condition and was made to a normal (.023%) sulfur level and a low (.006%) sulfur level. The Charpy impact and tensile properties were measured between  $-96^{\circ}$  and  $+23^{\circ}\text{C}$  ( $-141^{\circ}$  and  $+73^{\circ}\text{F}$ ). Static and dynamic fracture toughness using compact and bend specimens was measured over the same temperature range. Static  $K_{\text{IC}}$  was determined from  $J_{\text{IC}}$  at fracture, the  $J_{\text{IC}}$  at maximum load and from  $J$  vs  $4a$  curves. Dynamic  $K_{\text{ID}}$  was determined from the energy to fracture in an instrumented drop weight test.

The results of the tests show that both static and dynamic fracture toughness is improved by decreasing the sulfur content of the steel and by quenching and tempering rather than normalizing. Both the temperature of transition in toughness from low to high values and the absolute toughness level are improved. Static  $K_{\text{IC}}$  values ranged between 200 MPa and 280 MPa (about 180 Ksi to 250 Ksi) in the ambient temperature range and decreased to between 110 and 220 MPa/in (about 100 to 200 Ksi) at  $-96^{\circ}\text{C}$ . Dynamic fracture toughness, about equivalent to the static in the ambient range, decreases sharply at  $-40^{\circ}\text{C}$  ( $-40^{\circ}\text{F}$ ) and below.

## INTRODUCTION

When a new material is being developed for pressure vessel service, it is usually necessary to undertake a careful evaluation of the characteristics of the material before it is possible to establish the limits of its application and the specific benefits that it will provide. Such an evaluation will include determinations of strength, ductility and toughness over a range of temperature, fatigue behavior, response to heat treatment, weldability testing, and the effect of operating environment on these properties. While the material supplier or a potential user will often develop such data, it is also useful for an independent evaluation to be undertaken by a research organization that can bring to bear a wide range of experience on the evaluation. It was with this intent that the Pressure Vessel Research Committee of the Welding Research Council, through the Pressure Vessel Steels Subcommittee of the Materials Division, undertook in 1974 to begin the examination of a series of new steels for pressure vessel service. During the initial course of this investigation, portions of which were published as P.V.R.C. project reports,<sup>1,2</sup> relatively high strength steels were studied. In the more recent work, reported here, the properties of "microalloyed" carbon-manganese A 7 3 7 steels of moderate strength but much higher toughness are included in the program.

Evaluation of any new material involves not only measure-

ment of the normal material properties but also, in some cases, the development of new test procedures to provide the kind of information required. In the research reported here, both aspects of the problem were given attention. For the materials included in this investigation, the property of greatest importance is toughness, and thus adequate measures of toughness had to be considered and utilized. On the other hand, the measurement of toughness is still only a means to an end, as the ultimate usefulness of the material rests on the properties measured: thus, the overall intent of this work was to develop the anticipated properties of one of the newer A737 microalloyed steels and to do so with a fracture toughness test technique compatible with its inherent high toughness.

Fracture toughness testing to control the brittle fracture resistance of materials received its early development during and after the World War II period when the Charpy V-notch impact test was first utilized to establish the toughness of ship plate. Although empirical in nature, this test procedure has served for many years to provide a satisfactory fracture control parameter for ships, pressure vessel, and more recently bridges and some buildings. Current evaluations of fracture toughness for pressure vessel service still utilize this test; however, the pressure vessel industry as a whole has begun to use the principles of linear elastic fracture mechanics as an alternate method to establish the toughness required in these

structures. Fracture mechanics has been widely employed to interpret the fracture behavior of high strength steels (yield strength > 200 Ksi) for which plane strain behavior can be obtained at room temperature in relatively thin section sizes. As fracture mechanics analyses are extended to tougher, low strength steels, increased plasticity causes difficulties in the application of the linear elastic model to these materials.

The steel examined in this study, of which more will be said later, is an example of precisely the type of material for which analyses by linear elastic fracture mechanics is difficult. The relatively high ambient toughness and low yield strength of the steel makes measurement of fracture toughness by the linear elastic criteria and methods of ASTM standard E399 virtually impossible. This standard specifies that the thickness (and other dimensions) of the specimen to be used to measure the plane strain fracture toughness,  $K_{Ic}$ , must fulfill the inequality:

$$B \geq 2.5 \left( \frac{K_{Ic}}{\sigma_y} \right)^2 \quad \text{Eqn. 1}$$

where B is the specimen thickness and  $\sigma_y$  the yield point. Since the  $K_{Ic}$  is high relative to the yield point, not infrequently twice the yield point, the value of B is consequently very large, often on the order of 200-400mm (~8-16 in). Such a specimen size is not only impractical for testing, but often exceeds the thickness of the plate to be tested. Although the

steel selected for study in this investigation has a high level of toughness, it is by no means unique, because many pressure vessel steels have a ratio of  $K_{Ic}$  to  $\sigma_y$  which exceeds one in the service temperature range. In each of these cases the specimen thickness requirement becomes unrealistic, especially so when plate thicknesses are on the order of 25-75 mm (1-3 in).

The need to develop crack toughness measurement techniques which utilize smaller specimens became apparent more than fifteen years ago, and it was about ten years ago that serious work was done to provide an acceptable technique for performing and analyzing such tests. At the present time most of the efforts have used the same basic formulation as developed for linear elastic cases, i.e. a  $K_{Ic}$  is obtained experimentally and allowable stresses and/or flaw sizes determined from the experimental  $K_{Ic}$ . The difference lies in the fact that  $K_{Ic}$  is not measured directly but rather is estimated from an elastic-plastic crack toughness parameter measured on a small specimen. In this investigation, the  $K_{Ic}$  was estimated from the J-integral at the initiation of ductile tearing in a static compact specimen. Although other characterizations could have been used, the J-integral appears to give comparable results and has gained wide acceptance in the pressure vessel industry.

As is traditional for highly strain rate sensitive material, both static and dynamic toughness characterizations were desired and for this reason the  $K_{Id}$  was also determined.

Since the data obtained in these tests were not of the same type as the static tests, the  $K_{I_d}$  was estimated from the energy to fracture absorbed by bend specimens impacted with a falling weight. Both the static and dynamic test specimens were so designed that they could be analyzed by linear elastic fracture mechanics procedures in the low temperature regime. Some tests were performed at low enough temperatures that valid  $K_{I_c}$  data were obtained.

As indicated above, the material tested in this program is of importance in and of itself. It is one of a class of low-alloy high-strength steels that utilizes relatively low carbon content and finely dispersed carbides to provide a strength and toughness level that is suitable for low temperature service. This type of steel has been used for piping and structural applications under several different specifications but has only recently been incorporated into ASTM pressure vessel specifications such as A734, A735 and A737. The grade tested meets the ASTM A737 Grade B specification. The specified alloy element for strength is columbium. The plates were 100 mm (24 in) thick.

Because the aim of this study was to fully characterize this type of steel, several variations on the basic chemical composition and heat treatment were employed. First, the steel was provided in both the mill normalized and mill quenched and tempered condition. Second, the steel was provided in several



heats, two made to a normal sulfur level, about 0.025%, and one to a low sulfur level, less than 0.010%. The intent of these variations was to produce steel with a range of fracture toughness at low temperatures, some conditions being quite high in toughness and others being more normal for a low carbon, high manganese steel. Previous experience with carbon-manganese steels has shown that both quenching and tempering and control of sulfur contents to low levels are beneficial to Charpy impact toughness, the former lowering transition temperature and the latter raising upper shelf toughness. In this study, the aim was to determine the effect of these variables on typical fracture-mechanics parameters other than Charpy impact toughness. Thus the fracture toughness of all four conditions was determined over a range of temperatures, the final result being a comparison between the materials over the potential temperature range of service.

## TEST MATERIALS

The materials under investigation were microalloyed C-Mn ASTM A737 Grade B steel having the chemical composition and mechanical properties listed in Table 1. Since the primary aim of this investigation was the toughness of the steel, mechanical properties were determined in the worst or transverse (T-L) orientation. The steel was studied in four variations including two normal sulfur heats, 0.023%, (Table 1) and one low sulfur heat, 0.006%, (Table 2). Both types were studied in the mill quenched and tempered and the mill normalized conditions. The plates were nominally 100 mm (4 in) thick. The steel was produced by the electric arc process using a cold scrap charge. The low sulfur heat was calcium treated. Rolling was by conventional practice. The plates were austenitized at 900°C (1650°F) and either cooled in still air for normalizing or water sprayed and tempered at 595°C (1100°F) for quenching and tempering.

## TESTING PROCEDURES

### Tension and Charpy Impact Tests

Standard 6.35 mm (0.250 in) diameter button head specimens in the transverse (T-L) and longitudinal (L-T) orientations were tested at room and low temperatures according to ASTM specification A370. A 44.4 kN (10,000 lb) Instron testing machine with a constant crosshead speed of 5 mm/min (0.2 in/min) was used. Low temperature tests were performed in a bath of 2-methylbutane cooled with liquid nitrogen. Charpy V-notch impact tests were performed on T-L quarter and center thickness specimens of plates from all four test conditions over a range of temperatures. A 325J (240 ft-lb) Satec model SI-1 testing machine was used and testing was done to the ASTM Specification E23. Specimens for the low temperature tests were cooled in a bath of 2-methylbutane and liquid nitrogen.

### Fracture Toughness Tests

Compact specimens in 50 mm (2 in) thickness were prepared in the T-L orientation, precracked and tested statically according to the provisions of ASTM specification E399. The specimen used is seen in Figure 1. The specimens were tested over a range of temperatures between 23°C and -96°C (73°F and -141°F). Because of the relatively high toughness of the steel in the ambient range, many of the tests were invalid. The invalid test specimens were evaluated using the J-integral approach. The  $J_I$  value for these specimens was estimated using the approximation:<sup>3</sup>

$$J = \frac{2\lambda A}{Bb}$$

Egn. 2

Here J is the J integral, A is the area under the load-load point deflection curve to the deflection of interest, B is the specimen thickness, b is the remaining uncracked ligament, and  $\lambda$  is a correction factor to allow for the tensile forces on the crack (primarily a function of  $a/w$ )<sup>4</sup>.

The static tests were run on a 553 KN (120,000 lb) Baldwin universal testing machine. The load-load line displacements were measured using a strain gage bridge mounted on a load cell in the loading train and on a clip-in displacement gage mounted on the specimen crack mouth. These data were recorded on a Hewlett-Packard X-Y recorder. The crack mouth displacements were subsequently converted to load-line displacements by assuming the crack faces rotate during testing around a point 0.45b from the crack tip into the ligament, b. The temperature of the specimen was measured and recorded using a copper-constantin thermocouple on the specimen surface and a Sargent strip chart recorder. Low temperature was achieved by spraying liquid nitrogen on the specimen surface with the specimen and grips in an insulated chamber. Test temperature was held 10-15 minutes prior to testing.

Four or five specimens were tested at each of the higher test temperatures with testing of each specimen discontinued after a predetermined (estimated) amount of crack growth was

achieved. After the specimen was loaded to the predetermined load or displacement, the specimen was unloaded and the crack position heat tinted by placing it in a furnace (in air) at 427°C (800°F) for two hours. The specimen was subsequently tested to failure and crack growth in the central portion of the specimen measured at three points and averaged to give the "crack growth",  $\Delta a$ , for the specimen. Both  $J$  vs  $\Delta a$  and maximum load  $J$ -integral data were measured. In order to increase the maximum load information, specimens tested at lower temperature and heat tinted were pulled to failure at higher temperature, thus providing crack growth information and maximum load data (at two different temperatures) with one specimen. Inherent in this procedure is the assumption that heat tinting did not materially affect the maximum load achieved in the specimen.

Determination of the fracture toughness,  $K_{IC}$ , was done using the  $J$  vs  $\Delta a$  curves constructed from the test data (Figures 12-18). In each case the  $J_{IC}$  for the initiation of ductile tearing was determined by fitting a line through the  $J$  vs  $\Delta a$  points and constructing a "blunting" line from the expression<sup>5</sup>:

$$J = 2\Delta a\sigma_f \quad \text{Eqn. 3}$$

Here  $J$  is the  $J$ -integral,  $\Delta a$  is the displacement and  $\sigma_f$  is the flow stress of the material. The value of  $\sigma_f$  is approximated as being midway between the yield stress and ultimate tensile strength of the steel. The blunting line represents specimen displacement associated with plastic flow, not tearing. When

the data deviate from this line, displacement associated with true fracture occurs. Thus the intersection of the blunting line (Egn. 3) and the curve through the remaining data defines the  $\Delta a$  at fracture initiation and thus the true  $J_{Ic}$ . The  $K_{Ic}$  is calculated from  $J_{Ic}$  by the expression

$$K_{Ic} = \sqrt{\frac{J_{Ic} E}{1-\nu^2}} \quad \text{Eqn. 4}$$

Here E is Young's modulus and  $\nu$  is Poissons ratio.

Dynamic fracture toughness tests were performed, using T-L orientation, 50 mm (2 in) thick, fatigue cracked bend test specimens prepared according to the geometry requirement of ASTM specification E399 and tested in an instrumented drop weight tester. The specimens were cooled in a methanol or 2-methylbutane and liquid nitrogen bath and tested within 10 seconds after removal from it. The specimen was held at temperature for at least 10 minutes prior to testing. Half round 25 mm (1 in) diameter drill rod pads were placed on the specimen at the impact point to decrease the load rise time and reduce inertial effects. A smooth load-line trace without evidence of ringing was generally obtained, as shown in Figure 2. The data was recorded using a solid state transient recorder with the stored load-time pulse subsequently replayed on an X-Y recorder.

The impacting tup was machined from a high toughness steel heat treated to a hardness level of  $R_c 50$ . The testing fixture

provides two point support on a 400 mm ( 16 in) span. A 182Kg (400 lb) free falling weight supported by an electromagnetic release mechanism provided the impact load.

The dynamic fracture toughness was calculated using the concept that the nonlinear critical strain energy release rate ( $J_{cd}$ ) is proportional to the area under the force-displacement curve up to the point of fracture initiation.<sup>6</sup> The critical dynamic stress intensity,  $K_{dt}$ , is then calculated from  $J_{cd}$  using equations 2 and 4, i.e.

$$K_{dt} = \sqrt{\frac{J_{cd} E}{1-\nu^2}} = \sqrt{\frac{2 W_m E}{bB 1-\nu^2}} \quad \text{Eqn. 5}$$

The work to maximum load,  $W_m$ , may be approximated by <sup>6</sup>:

$$W_m = \int_0^{x_m} P dx = \int_0^{t_m} P V dt = V_0 \int_0^{t_m} P dt \quad \text{Eqn. 6}$$

In this it is assumed that the work to maximum load,  $P_{max}$ , may be approximated from the load-time trace using the velocity at impact,  $V_0$ , and the time to failure,  $t_m$ . The  $V_0$  at impact is calculated from:

$$V_0 = 2gh \quad \text{Eqn. 7}$$

where  $h$  is the height the weight is released from and  $g$ , the acceleration due to gravity. At the lowest temperatures tested,  $-96^\circ\text{C}$  ( $-141^\circ\text{F}$ ), most of the specimens had flat fracture surfaces and the values obtained are believed to be valid in the

sense used in ASTM E399.

#### Metallographic Examination

The four material variations in the study were examined metallographically at centerline thickness in a longitudinal orientation plane. Standard polishing and etching procedures were employed with 2% nital used for the final etch. Photomicrography was done using a Zeiss Axiomat metallograph and Polaroid PNSS film.



## RESULTS AND DISCUSSION

### Tension and Impact Tests

The results of the tension tests on the four plates of A737 Grade B are listed in Table 3 and may be compared to the data of Tables 1 and 2. The same data are also plotted in Figures 3-5. As is evident from Table 3, all of the plates meet the minimum longitudinal (L-T) yield and tensile strength specifications for the grade. The quenched and tempered plates have higher yield and tensile strengths than their normalized counterparts, the most noticeable difference being in yield strength. The low sulfur plates appear higher in strength than the normal sulfur ones. This effect is probably due to the somewhat higher manganese and residual element content of this low sulfur heat rather than its sulfur content. Figures 3, 4, and 5 show that the yield and tensile strengths of the plates gradually increase with decreasing temperature. Between 23°C and -96°C (73°F and -141°F) the yield strength increases about 35% for the normalized material and about 30% for the quenched and tempered material. Tensile strengths increased about 25% over the same temperature range, the increase for the normalized steel again being somewhat greater. Tensile ductility shows a modest increase over the temperature range tested, except for the low sulfur heat where a slight loss is noted at -96°C (-141°F).

The impact test results are shown in Figures 6-9.

Although all four of the plates show good impact toughness at temperatures down to at least  $-50^{\circ}\text{C}$  (about  $-60^{\circ}\text{F}$ ), the low sulfur plates are clearly superior in transition temperature and have a substantially higher upper shelf toughness. The improved shelf toughness is one of the chief benefits of low sulfur steels, and this is graphically illustrated in these cases. For each sulfur level, the quenched and tempered steel is lower in transition temperature and higher in shelf energy, although this effect is not as marked as the effect of decreased sulfur. When reviewing these figures, it should be emphasized that transverse (T-L) specimen data are being shown. Longitudinal specimen data would probably give somewhat higher toughness values. Center and quarter thickness specimen data are shown on Figures 6-9. The difference in toughness between specimens taken from these two locations is slight. In only one case does the quarter thickness location give higher toughness

#### Metallography

The microstructure of the four plates seen in Figures 10 and 11 appears to be generally consistent with the results of the tensile and Charpy impact tests. The quenched and tempered plates have much finer ferrite-carbide aggregates than the normalized ones, but are otherwise similar in structure. As might be expected, the hardenability of the steel is insufficient to form lower temperature transformation products; however

a substantial structural refinement occurs and is relatively uniform across the central two-thirds of the plate. The improvement in yield and tensile strength with quenching and tempering is undoubtedly a result. As indicated before, a decrease in transition temperature and an increase in shelf toughness results from this refinement.

From the standpoint of overall structure and uniformity, the low sulfur heat is, as expected, cleaner, i.e. has fewer inclusions. The inclusions that are present tend to be more rounded. However, it is also observable that the low sulfur heat has more pronounced ferrite-pearlite banding. The banding appears more pronounced in normalized than in the quenched and tempered condition. It is possible that the relatively high manganese content of this heat may have contributed to the banding tendency. Because of the nature of this experiment it is impossible to determine what effect, if any, the banding has on mechanical properties.

#### Static Fracture Toughness

The static fracture toughness data for the A737 Grade B steel are found in Tables 4 and 5. The  $J_{IC}$  data obtained for each condition are of three types. At low temperatures, generally  $-96^{\circ}$  to  $-100^{\circ}\text{C}$  ( $-141^{\circ}$  to  $-148^{\circ}\text{F}$ ), the values listed as  $J_{IC}$  are based on a distinct fracture load. Because of the thickness of the specimen, they are not valid by the specifications of ASTM E399. The  $J_{IC}$  was therefore determined for

these cases from the area of the P- $\Delta$  curve to fracture. At higher temperatures, no distinct fracture was observed. In these cases, the J vs  $\Delta a$  curve was constructed. These curves are found in Figures 12-18. A  $J_{IC}$  was determined from the blunting line-data curve intersection. In addition, the single curve from the J vs  $\Delta a$  data set which had a deflection that extended to maximum load was selected and a  $J_{IC}$  was calculated at maximum load for this sample. The summary column of  $K_{IC}$  is calculated from the  $J_{IC}$  using Eqn. 4 with the nature of the data indicated by a subscript, i.e. based on fracture, maximum load deflection or the J vs  $\Delta a$  curve.

The J vs  $\Delta a$  curves, Figures 12-18, proved to be relatively smooth with most of the data lying close to a straight line. In several cases, the data could have just as well fitted some other function. Data in the literature are occasionally plotted nonlinearly, but since there was no clear precedent for this, a straight line mechanical fit of the data was chosen here. The resulting  $J_{IC}$  values determined from the intersection points were generally self consistent. For example, the  $K_{IC}$  values for the low sulfur heat determined by this method were 234 MPa/m (213 Ksi/in) and 241 MPa/m (219 Ksi/in) at -46° and 23°C (-51° and 73°F), respectively, for the normalized condition. The quenched and tempered condition data were 275 MPa/m (251 Ksi/in) and 279 MPa/m (254 Ksi/in) at the same two temperatures. The relatively small effect of temper-

ature is consistent with the fact that the material is on the upper shelf of toughness over this temperature range in static tests. By way of comparison, the normal sulfur heats, which had a lower shelf toughness in the Charpy tests, had a  $K_{IC}$  of 198 MPa $\sqrt{m}$  (181 Ksi $\sqrt{in}$ ) and 237 MPa $\sqrt{m}$  (215 Ksi $\sqrt{in}$ ) at 23°C (73°F) for the normalized and the quenched and tempered condition, respectively. At low temperatures, -96°C (-141°F) the materials rank in the same order, although the  $J_{IC}$  is determined in this case from a definite fracture criterion in the test. The low sulfur steel once again had higher values of  $K_{IC}$  in both conditions than the corresponding normal sulfur heat. For each sulfur level, the quenched and tempered value was greater than the normalized one. A summary of the  $K_{IC}$  values on Tables 4 and 5 is shown in Figure 19.

Of some practical interest from the standpoint of testing is a comparison of the  $K_{IC}$  calculated from  $J_{IC}$  at maximum load and that calculated from the  $J_{IC}$  intersection point on the J vs  $\Delta a$  curves. From Tables 4 and 5 it can be seen that the maximum load  $K_{IC}$  is consistently larger than that from the J vs  $\Delta a$  curves, the intersection point  $K_{IC}$  being between 5% and 20% smaller. This implies that ductile tearing in this steel always precedes the maximum load point in the test and suggests that a simplified test technique could be used. The maximum load  $J_{IC}$  could be determined for the material using one or several specimens and a  $K_{IC}$  calculated. This value could then be reduced by 20% to give the approximate  $K_{IC}$  at

the initiation of tearing.

#### Dynamic Fracture Toughness

The dynamic fracture toughness data are found in Tables 6 and 7 where  $K_d$  based on maximum load and  $K_{dt}$  from Eqn. 5 are both listed.  $K_{dt}$  values are plotted on Figure 20. It is apparent that at ambient temperatures for the normal sulfur level steel, the dynamic fracture toughness level is about equal to that of the static. At lower temperatures, however, starting at 0°C (32°F) for the normalized material and at -45°C (-48°F) for the quenched and tempered, the fracture toughness decreases sharply. For temperatures at -45°C (-48°F) and below, valid  $K_{Ic}$  data are obtained using the maximum load in the test. At higher temperature the  $K_{dmax}$  values are not meaningful. This result is somewhat surprising as the Charpy impact data indicate a relatively high toughness in the same temperature range; however, it is not inconsistent with the relationship between static and dynamic fracture toughness test data found in the literature. The temperature shift,  $T_s$ , between static and dynamic  $K_{Ic}$  data has been shown to be a function of the material yield point,  $\sigma_y$ , as follows<sup>7</sup>:

$$T_s(^{\circ}\text{F}) = 215 - 1.5\sigma_y (K_{si}) \quad \text{Eqn. 7}$$

For the normal sulfur material studied here, the yield point is between 345 and 415 MPa (50 and 60 Ksi) and thus the shift should be between 70° and 80°C (125° and 145°F). This

is, in fact, in agreement with the data from Figures 19 and 20 in that a  $K_{Ic}$  for the normalized steel of about  $150 \text{ MPa}\sqrt{\text{m}}$  ( $136 \text{ Ksi}\sqrt{\text{in}}$ ) occurs at about  $-70^\circ\text{C}$  ( $-94^\circ\text{F}$ ) while the  $K_{Id}$  of the same value is at about  $10^\circ\text{C}$  ( $50^\circ\text{F}$ ), a shift of  $80^\circ\text{C}$ . The corresponding shift for the quenched and tempered steel is also about  $80^\circ\text{C}$ . These shifts can readily be seen on the summary curves, Figures 21 and 22. The difference between the Charpy impact results and the 50 mm (2 in) thick specimen data would then have to be attributed to a specimen size effect.

#### Fracture Toughness Summary

The fracture toughness data obtained in this investigation are summarized in Figures 21 and 22 for the normal and low sulfur A737B steel. The curves are plotted from the  $J$  vs  $\Delta a$  intersection data and fracture  $K_{Ic}$  data on Tables 4 and 5, as well as the dynamic  $K_{dt}$  data on Tables 6 and 7. An alternate approach to summarizing the fracture data obtained in this program could be to present the results on the basis of "crack toughness" rather than the fracture toughness alone<sup>8</sup>. The crack toughness parameter of greatest usefulness is the ratio of  $K_{Ic}$  to  $\sigma_y$ . This ratio is a fundamental measure of the plastic zone size at a crack tip during fracture and also, therefore, a measure of the plate thickness necessary for plane strain conditions at fracture. It appears in Eqn. 1 in this respect, and since it is a squared term, it exerts a significant influence. The data from Figures 21 and 22 are replotted

in Figures 23 and 24 utilizing this approach. For this analysis the dynamic yield point was estimated by adding 175 MPa (25 Ksi) to the static yield point at temperature. This is based on the elevation of the yield point by 35 MPa for each order of magnitude increase in strain rate between the two conditions.

On this basis, for example, plane strain conditions do not prevail for any material at any temperature examined in this program for plates up to 125 mm (5 in) thick in the static mode of loading. In the ambient range, static plane strain plate thicknesses exceed 765 mm (30 in). Dynamic plane strain plate thicknesses in the ambient range are on the order of 330 mm (13 in). In temperature range of  $-50^{\circ}\text{C}$  ( $-68^{\circ}\text{F}$ ) dynamic plane strain plate thicknesses are much smaller because the  $K_{Id}$  is generally smaller than the  $K_{Ic}$  and the effective yield strength is elevated by strain rate. In spite of this effect, at temperatures above  $-40^{\circ}\text{C}$  ( $-40^{\circ}\text{F}$ ) dynamic plane strain plate thicknesses are over 46 mm (1.0 in) with the exception of the normalized, normal sulfur heat. At very low temperatures, dynamic plane strain thicknesses decrease to 2-8 mm (.08 to .32 in).



## CONCLUSIONS

From this investigation of the static and dynamic toughness of A737 Grade B steel in two conditions of heat treatment and at two levels of sulfur content, the following was concluded:

1. In terms of both Charpy impact transition temperature and Charpy impact upper shelf toughness, the low sulfur (.006%) heat of A737 B held a decided advantage over the normal sulfur (0.023%) heats. The transition temperature of the low sulfur heat was at least 30°C (54°F) lower than that of the normal sulfur heats and the shelf toughness about 100% higher. The quenched tempered condition plates were between 10° and 20°C (18° and 36°F) lower in transition temperature than their normalized counterparts. Shelf toughnesses were nearly equivalent for the two conditions.
2. In terms of static plane strain fracture toughness, the low sulfur heat was again higher in toughness than the normal sulfur heats over the range of temperatures tested, the difference between the two being about 20%. The quenched and tempered plates were also superior to the normalized ones for each sulfur level by about 20%.  $K_{Ic}$  values ranged between 200 MPa to 280 MPa (about 180Ksi to 250 Ksi) at ambient temperatures for the four conditions and between 110 and 220 MPa/m (about 100 and 200 Ksi) at -96°C (-141°F). Fracture toughness determined from the

$J_{Ic}$  at maximum load were higher than those determined from  $J$  vs  $\Delta a$  curves, the difference varying between 5 and 25%.

3. The dynamic fracture toughness for the plates tested was lower than the static values except in the ambient range. The same basic trends with regard to sulfur level and the effect of heat treatment on toughness seen in the static tests were followed in the dynamic ones, although the percentage differences were more variable. Plane strain fracture toughness values in 50 mm (2 in) specimens were obtained below  $-40^{\circ}\text{C}$  ( $-40^{\circ}\text{F}$ ) for the normalized plates and at  $-96^{\circ}\text{C}$  ( $-141^{\circ}\text{F}$ ) for the quenched and tempered ones. The shift of the toughness vs temperature curve as a result of the strain rate increase between the static and dynamic tests was about  $80^{\circ}\text{C}$  ( $145^{\circ}\text{F}$ ).
4. An analysis of the A737 Grade B steel in terms of the  $K_{Ic}$  to  $\sigma_y$  ratio shows that, in the ambient range, plane strain plate thicknesses are greater than 330 mm (13 in) for any condition tested. Plane strain plate thicknesses for static loading conditions remain above this level down  $-96^{\circ}\text{C}$  ( $-141^{\circ}\text{F}$ ). Plane strain plate thicknesses under dynamic loading decrease sharply at  $-40^{\circ}\text{C}$  ( $-40^{\circ}\text{F}$ ) and below, with values at  $-40^{\circ}\text{C}$  ( $-40^{\circ}\text{F}$ ) ranging from about 25 to 75 mm (1 to 3 in) and at  $-96^{\circ}\text{C}$  ( $-141^{\circ}\text{F}$ ), from about 2 to 8 mm (.1 to .3 in).

TABLE 1

Chemistry and Mechanical Property Data for A737B Steel - Normal Sulfur\*

A. Chemical Composition

<u>Plate</u>	<u>C</u>	<u>Mn</u>	<u>P</u>	<u>S</u>	<u>Si</u>	<u>Ni</u>	<u>Cr</u>	<u>Mo</u>	<u>Cu</u>	<u>Al</u>	<u>Cb</u>
Normalized	.16	1.27	.007	.023	.22	.14	.15	.04	.26	.036	.033
Quenched & Tempered	.16	1.16	.012	.022	.19	.13	.14	.05	.25	.030	.025

B. Tension Test Properties (Transverse)

<u>Plate</u>	<u>Yield Strength</u>		<u>Tensile Strength</u>		<u>Elong.</u>	<u>R.A.</u>
	<u>MPa</u>	<u>(Ksi)</u>	<u>MPa</u>	<u>(Ksi)</u>	<u>%</u>	<u>%</u>
Normalized	312	(45.4)	504	(73.1)	32.4	71.5
Quenched & Tempered	388	(56.3)	518	(75.0)	34.0	74.9

C. Charpy Impact Test Properties (Transverse)

<u>Plate</u>	<u>50 ft-lb (67.5J)</u>	<u>Transition Temp.</u>	<u>Upper Shelf Energy</u>	
	<u>°C</u>	<u>(°F)</u>	<u>J</u>	<u>(ft-lb)</u>
Normalized	-29	(-20)	122	(90)
Quenched & Tempered	-56	(-70)	143	(105)

\*Data provided by Lukens Steel Company

TABLE 2

Chemistry and Mechanical Property Data for A737B Steel - Low Sulfur\*

A. Chemical Composition

<u>Plate</u>	<u>C</u>	<u>Mn</u>	<u>P</u>	<u>S</u>	<u>Si</u>	<u>Ni</u>	<u>Cr</u>	<u>Mo</u>	<u>Cu</u>	<u>Al</u>	<u>Q</u>
Normalized & Quenched & Tempered	.14	1.44	.009	.006	.19	.28	.22	.09	.27	.030	.025

B. Tension Test Properties (Transverse)

<u>Plate</u>	<u>Yield Strength</u>		<u>Tensile Strength</u>		<u>Elong.</u> <u>%</u>	<u>R.A.</u> <u>%</u>
	<u>MPa</u>	<u>(Ksi)</u>	<u>MPa</u>	<u>(Ksi)</u>		
Normalized	389	(56.4)	546	(79.3)	29	58.1
Quenched & Tempered	436	(63.3)	577	(83.7)	27.5	67.5

C. Charpy Impact Test Properties (Transverse)

	<u>Energy at Temperature - Joules (ft-lb)</u>		
	<u>(-50°F)</u>	<u>(-80°F)</u>	<u>(-100°F)</u>
Normalized	147 (109)	144 (107)	123 (91)
Quenched & Tempered	154 (114)	-	-

\*Data provided by Lukens Steel Company

**TABLE 3**  
Tension Test Data for A737B Steel

Plate, Orientation and Heat Treatment	Temperature C (°F)	Yield St. MPa (Ksi)	Tensile St. MPa (Ksi)	Elongation %
Normal Sulfur, Longitudinal, Normalized	22 (72)	351 (51.0)	505 (73.3)	38.1
	-46 (-50)	395 (57.3)	575 (83.4)	36.5
	-96 (-140)	482 (69.9)	643 (93.3)	38.1
Normal Sulfur, Transverse, Normalized	22 (72)	354 (51.4)	500 (72.5)	34.2
	-46 (-50)	373 (54.2)	576 (83.6)	38.8
	-96 (-140)	463 (67.2)	639 (92.8)	37.1
Normal Sulfur, Longitudinal, Quenched & Tempered	22 (72)	407 (59.1)	492 (71.4)	36.5
	-46 (-50)	465 (67.5)	591 (85.8)	36.6
	-96 (-140)	522 (75.8)	641 (93.1)	-
Normal Sulfur, Transverse, Quenched & Tempered	22 (72)	400 (58.1)	542 (78.6)	34.1
	-46 (-50)	391 (56.7)	560 (81.3)	36.5
	-96 (-140)	523 (75.9)	662 (96.1)	34.0
Low Sulfur, Longitudinal, Normalized	22 (72)	368 (53.4)	531 (77.0)	36.9
	-46 (-50)	451 (65.5)	630 (91.4)	38.6
	-96 (-140)	520 (75.2)	688 (99.8)	39.1
Low Sulfur, Transverse, Normalized	22 (72)	366 (53.1)	513 (74.5)	36.5
	-46 (-50)	432 (62.7)	606 (88.0)	40.0
	-96 (-140)	506 (73.4)	693 (100.6)	40.8
Low Sulfur, Longitudinal, Quenched & Tempered	22 (72)	444 (64.5)	568 (82.5)	31.1
	-46 (-50)	506 (73.5)	652 (94.6)	32.9
	-96 (-140)	586 (85.0)	722 (104.8)	32.6
Low Sulfur, Transverse, Quenched & Tempered	22 (72)	469 (68.0)	576 (83.6)	29.2
	-46 (-50)	545 (79.1)	681 (98.9)	32.1
	-96 (-140)	613 (89.0)	731 (106.1)	32.5

TABLE 4  
 Static Fracture Toughness Results for A737 Grade B  
 Normal Sulfur Heats - Transverse

Specimen No.	Temperature		J <sub>a</sub> mm (mils)	J KJ/m <sup>2</sup> (in-lb/in <sup>2</sup> )	J <sub>IC</sub> KJ/m <sup>2</sup> (in-lb/in <sup>2</sup> )		K <sub>IC</sub> MPa√m (Ksi√In)	
	°C	(°F)						
Normalized								
NC-1	23	( 73 )		102	( 584 )			
ND-1	23	( 73 )	0.015	( 0.6 )	134	( 768 )		
NB-1	23	( 73 )	0.05	( 2 )	141	( 804 )		
NB-3	23	( 73 )	0.27	( 11 )	187	( 1068 )	197	( 1068 )*
NA-2	23	( 73 )	0.83	( 33 )	274	( 1562 )		
NB-2	23	( 73 )	20	( 80 )	394	( 2250 )		
Graph	23	( 73 )					170	( 975 ) <sup>+</sup>
N-1	-50	( -58 )			109	( 626 ) <sup>#</sup>	109	( 626 ) <sup>#</sup>
NC-3	-50	( -58 )			240	( 1369 ) <sup>#</sup>	240	( 1369 ) <sup>#</sup>
NA-3	-96	( -140 )			43	( 248 ) <sup>#</sup>	43	( 248 ) <sup>#</sup>
NC-2	-100	( -148 )			57	( 327 ) <sup>#</sup>	57	( 327 ) <sup>#</sup>
Quenched and Tempered								
4-2-CI	23	( 73 )			93	( 534 )		
4-2-D2	23	( 73 )	0.08	( 3.3 )	211	( 1202 )		
QT 1	23	( 73 )	0.38	( 15 )	270	( 1531 )		
4-2-B2	23	( 73 )	0.49	( 19 )	287	( 1635 )	287	( 1635 )*
4-2-5	23	( 73 )	1.55	( 62 )	395	( 2255 )		
4-2-6	23	( 73 )	2.25	( 90 )	512	( 2922 )		
Graph	23	( 73 )					240	( 1375 ) <sup>+</sup>
4-2-C3	-41	( -42 )	0.01	( 0.4 )	127	( 726 )		
4-2-B1	-41	( -42 )	0.08	( 3 )	242	( 1379 )		
4-2-D1	-41	( -42 )	0.46	( 18 )	360	( 2054 )	350	( 2054 )*
QT 2	-41	( -42 )	1.88	( 75 )	456	( 2620 )		
4-2-8	-41	( -42 )	1.425	( 57 )	383	( 2183 )		
4-2-9	-41	( -42 )	1.25	( 50 )	381	( 2171 )		
Graph	-41	( -42 )					227	( 1300 ) <sup>+</sup>
4-2-A3	-96	( -140 )			118	( 676 ) <sup>#</sup>	118	( 676 ) <sup>#</sup>
4-2-C2	-100	( -148 )			73	( 420 ) <sup>#</sup>	73	( 420 ) <sup>#</sup>

\* Max Load Value  
 + Intersection Point on Figures  
 # Max Load Value - Fracture

TABLE 5

Static Fracture Toughness Data for A737 Grade B  
Low Sulfur Heat - Transverse

Specimen No.	Temperature °C (°F)	$a$ mm (in)	J $KJ/m^2$ (in-lb/in <sup>2</sup> )	$J_{Ic}$ $KJ/m^2$ (in-lb/in <sup>2</sup> )	$K_{Ic}$ $MPa\sqrt{m}$ (ksi/in)
<b>Normalized</b>					
SB-A3	23 ( 73 )	0.21 ( 8 )	250 (1425)		
SB-A1	23 ( 73 )	0.46 (18)	289 (1650)		
SB-A2	23 ( 73 )	0.75 (30)	410 (2339)	410 (2239)*	301 (274)*
SB-D1	23 ( 73 )	0.77 (31)	432 (2464)		
Graph	23 ( 73 )			250 (1425)*	241 (219)*
SB-D3*	-46 (-51)		292 (1508)	282 (1608)*	256 (232)*
SB-B3	-46 (-51)	0.162(65)	227 (1295)		
SB-D2	-46 (-51)	0.42 (17)	317 (1808)		
SB-B2	-46 (-51)	0.65 (26)	414 (2360)		
Graph	-46 (-51)			236 (1350)*	234 (213)*
SB-C2	-96 (-141)		76 ( 435)*	76 ( 435)* <sup>‡</sup>	147 (134)* <sup>‡</sup>
<b>Quenched and Tempered</b>					
SA-B1	23 ( 73 )	0.37 (15)	369 (2106)	369 (2106)*	292 (266)*
SA-D2	23 ( 73 )	0.40 (16)	320 (1824)		
SA-D3	23 ( 73 )	0.50 (20)	403 (2297)		
SA-D1	23 ( 73 )	1.20 (48)	566 (3237)		
Graph	23 ( 73 )			336 (1925)*	279 (254)*
SA-C2	-46 (-51)	0.32 (13)	365 (2031)		
SA-B2	-46 (-51)	0.50 (20)	443 (2524)		
SA-C1	-46 (-51)	0.52 (25)	519 (2961)	519 (2961)*	346 (315)*
SA-B3	-46 (-51)	0.87 (35)	613 (3494)		
Graph	-46 (-51)			328 (1875)*	275 (251)*
SA-A1	-96 (-140)		226 (1291)	226 (1291)* <sup>‡</sup>	229 (208)* <sup>‡</sup>
SA-C3	-96 (-140)		250 (1426)	250 (1426)* <sup>‡</sup>	240 (218)* <sup>‡</sup>

\* Max Load Value

+ Intersection Point On Figures

‡ Max Load Value - Fracture

TABLE 6

Dynamic Fracture Toughness Data For A737 Grade B Steel  
Normal Sulfur Heats - Transverse

Specimen No.	Temperature °C (°F)	Fracture Mode	$K_{Ic}$ (max) E399 MPa√m (KSI√in)	$W_p$ Joules (Fr. Lbs.)	$K_{Ic}$ MPa√m (KSI√in)
Normalized					
N-8	23 ( 73)	1	100 ( 91)		
4-1	23 ( 73)	1	163 ( 148)	3318 (2447)	211 (192)
4-1-5	23 ( 73)	1	147 ( 134)	2957 (2181)	200 (182)
Avg.	23 ( 73)	1	136 ( 124)	3138 (2314)	205 (197)
4-1-1	0 ( 32)	1	136 ( 124)	198 ( 146)	54 ( 49)
4-1-6	0 ( 32)	1	131 ( 120)	717 ( 529)	101 ( 92)
Avg.	0 ( 32)	1	134 ( 122)	( 337)	( 77)
N-3	-10 ( 14)	1	111 ( 100)	493 ( 364)	93 ( 75)
N-6	-45 ( -48)	2	68* ( 62)	164 ( 121)	47 ( 43)
4-1-10	-45 ( -48)	2	53* ( 49)		
Avg.	-45 ( -48)	2	51* ( 47)	154 ( 121)	47 ( 43)
N-2	-70 ( -94)	2	35* ( 32)	102 ( 75)	32 ( 29)
N-1	-96 ( -141)	2	32* ( 29)	35 ( 26)	37 ( 34)
4-1-12	-96 ( -141)	2	42* ( 41)		
Avg.	-96 ( -141)	2	36* ( 33)	35 ( 26)	37 ( 34)
Quenched & Tempered					
Q-T-1	23 ( 73)	3	109 ( 99)		
4-2-11	23 ( 73)	1	177 ( 161)	3570 (2633)	219 (200)
4-2-12	23 ( 73)	1	127 ( 115)	2231 (1645)	190 (173)
Avg.	23 ( 73)		135 ( 125)	2900 (2139)	203 (193)
4-2-3	0 ( 32)	1	156 ( 171)	2251 (1660)	175 (159)
4-2-5	0 ( 32)	1	162 ( 175)	2551 (1892)	186 (169)
Avg.	0 ( 32)		159 ( 173)	2401 (1771)	180 (164)
QT-5	-10 ( 14)	1	129 ( 117)		
QT-8	-45 ( -48)	1	98 ( 89)	823 ( 607)	105 ( 96)
42-10	-45 ( -48)	1	109 ( 99)	593 ( 504)	97 ( 88)
Avg.	-45 ( -48)		103 ( 94)	752 ( 555)	102 ( 92)
QT-2	-70 ( -94)	2	38* ( 34)	57 ( 42)	28 ( 25)
QT-7	-96 ( -141)	2	26* ( 24)	35 ( 26)	22 ( 20)
4-2-9	-96 ( -141)	2	41* ( 37)		
Avg.	-96 ( -141)		33* ( 30)	35 ( 26)	22 ( 20)

1 Ductile Fracture

2 Brittle Fracture

3 Crack Did Not Propagate

\* Valid  $K_{Ic}$  By Specimen Size Criterion



TABLE 7

Dynamic Fracture Toughness Data for A737 Grade B Steel  
Low Sulfur Heats - Transverse

Specimen No.	Temperature °C	Temperature (°F)	Fracture Mode	$K_{D(max)}$ E399 MPa/m (Ksi in)	$W_m$ Joules(ft-lbs)	$K_{Dt}$ MPa/m (Ksi/in)
<b>Normalized</b>						
5B-4	23	(73)	1	192 (175)	5256 (3882)	268 (244)
5B-7	-45	(-48)	1	145 (132)	306 (226)	67 (61)
5B-8	-45	(-48)	1	156 (141)	841 (620)	105 (96)
Avg.	-45	(-48)		150 (136)	573 (423)	86 (78)
5B-1	-96	(-141)	2	93* (85)		
5B-2	-96	(-141)	2	90* (82)	104 (77)	38 (35)
Avg.	-96	(-141)		92* (83)	104 (77)	38 (35)
<b>Quenched &amp; Tempered</b>						
5A-5	23	(73)	1	221 (202)	3141 (2327)	222 (203)
5A-6	23	(73)	1	199 (182)	3250 (2397)	222 (203)
Avg.	23	(73)		210 (192)	3195 (2362)	222 (203)
5A-7	-45	(-48)	1	119 (108)	697 (514)	98 (89)
5A-8	-45	(-48)	1	137 (125)		
Avg.	-45	(-48)		128 (116)	697 (514)	98 (89)
5A-1	-96	(-141)	2	90* (82)	150 (111)	45 (41)
5A-2	-96	(-141)	2	94* (86)	125 (92)	42 (38)
Avg.	-96	(-141)		92* (84)	138 (101)	43 (39)

1 Ductile Fracture

2 Brittle Fracture

\* Valid  $K_{Id}$  by Specimen Size Criterion

TABLE 8

Summary of Fracture Toughness Data for A737 Grade B Steel  
Transverse Properties

Material & Condition	Temperature		$K_{Ic}$ MPa/m(Ksi/in)	$K_{dt}$ MPa/m(Ksi/in)	$K_{Ic}/\sigma_y$ √in	$K_{dt}/\sigma_y$ √in	Plain Strain Thick	
	°C (°F)	Normal Sulfur					Static m.s. (in)	Dynamic mm (in)
Normal Sulfur	23 ( 73)	Normal Sulfur	199 (181)	205 (187)	3.54	2.46	785 (31)	380 (15)
	-41 (-42)		198 (180)	47 ( 43)	3.33	0.61	710 (28)	24 (.9)
	-96 (-141)		108 ( 98)	37 ( 34)	1.46	0.36	135 ( 5)	8 (.3)
Quenched & Tempered	23 ( 73)	Quenched & Tempered	237 (215)	204 (186)	3.71	2.24	865 (34)	330 (13)
	-41 (-42)		230 (209)	101 ( 92)	3.67	1.12	865 (34)	80 ( 3)
	-96 (-141)		149 (135)	22 ( 20)	1.77	0.20	200 ( 8)	3 (.1)
Low Sulfur	23 ( 73)	Low Sulfur	241 (219)	266 (244)	4.13	3.12	1090 (43)	618 (24)
	-45 (-49)		234 (213)	86 ( 78)	3.38	0.89	735 (29)	51 ( 2)
	-96 (-141)		147 (134)	38 ( 35)	1.83	0.36	215 ( 8)	8 (.3)
Quenched & Tempered	23 ( 73)	Quenched & Tempered	307 (279)	222 (203)	4.10	2.18	1065 (42)	305 (12)
	-45 (-49)		303 (273)	98 ( 89)	3.48	0.86	760 (30)	46 ( 2)
	-96 (-141)		234 (213)	43 ( 39)	2.39	0.18	355 (14)	2 (.1)

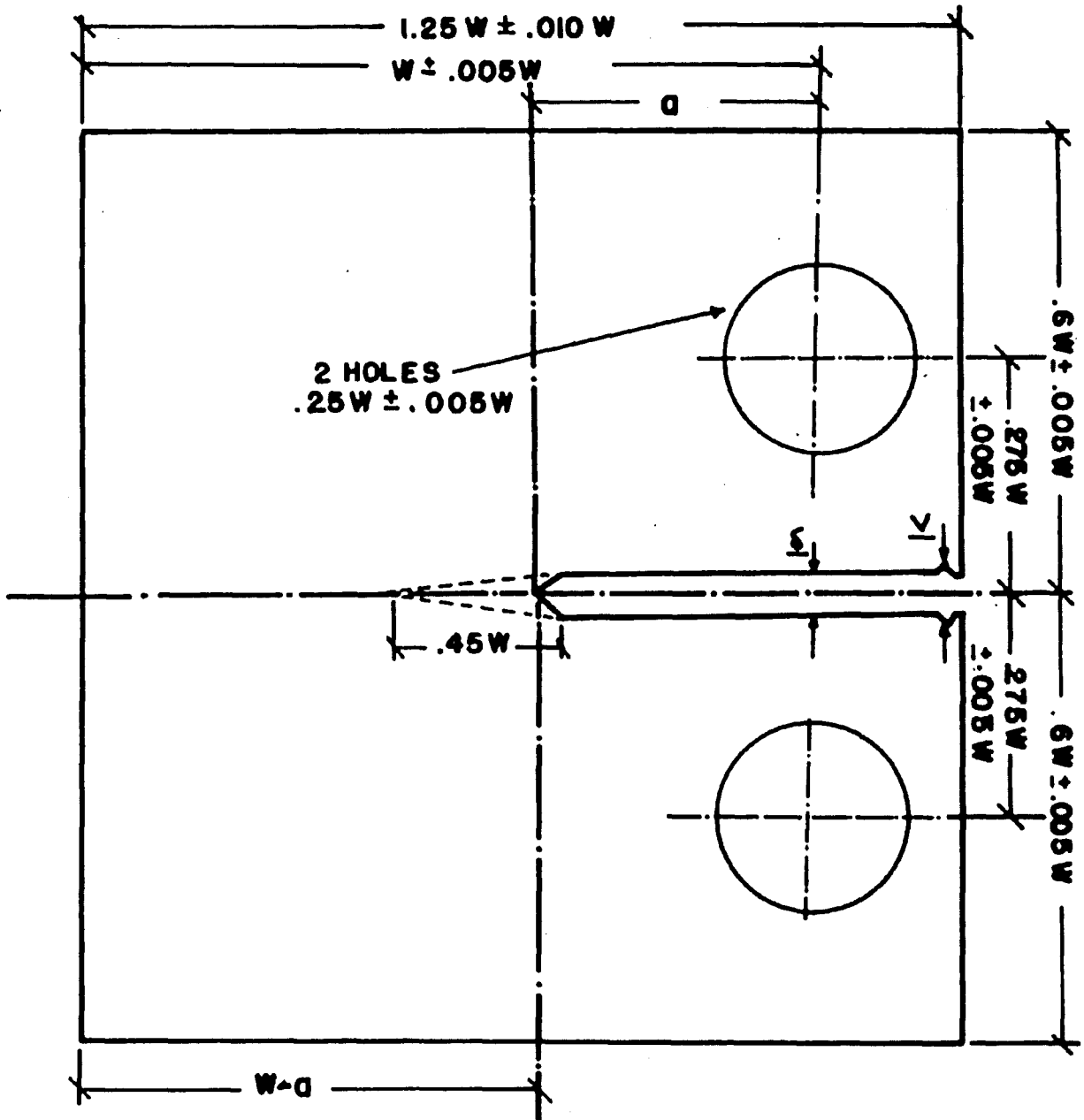
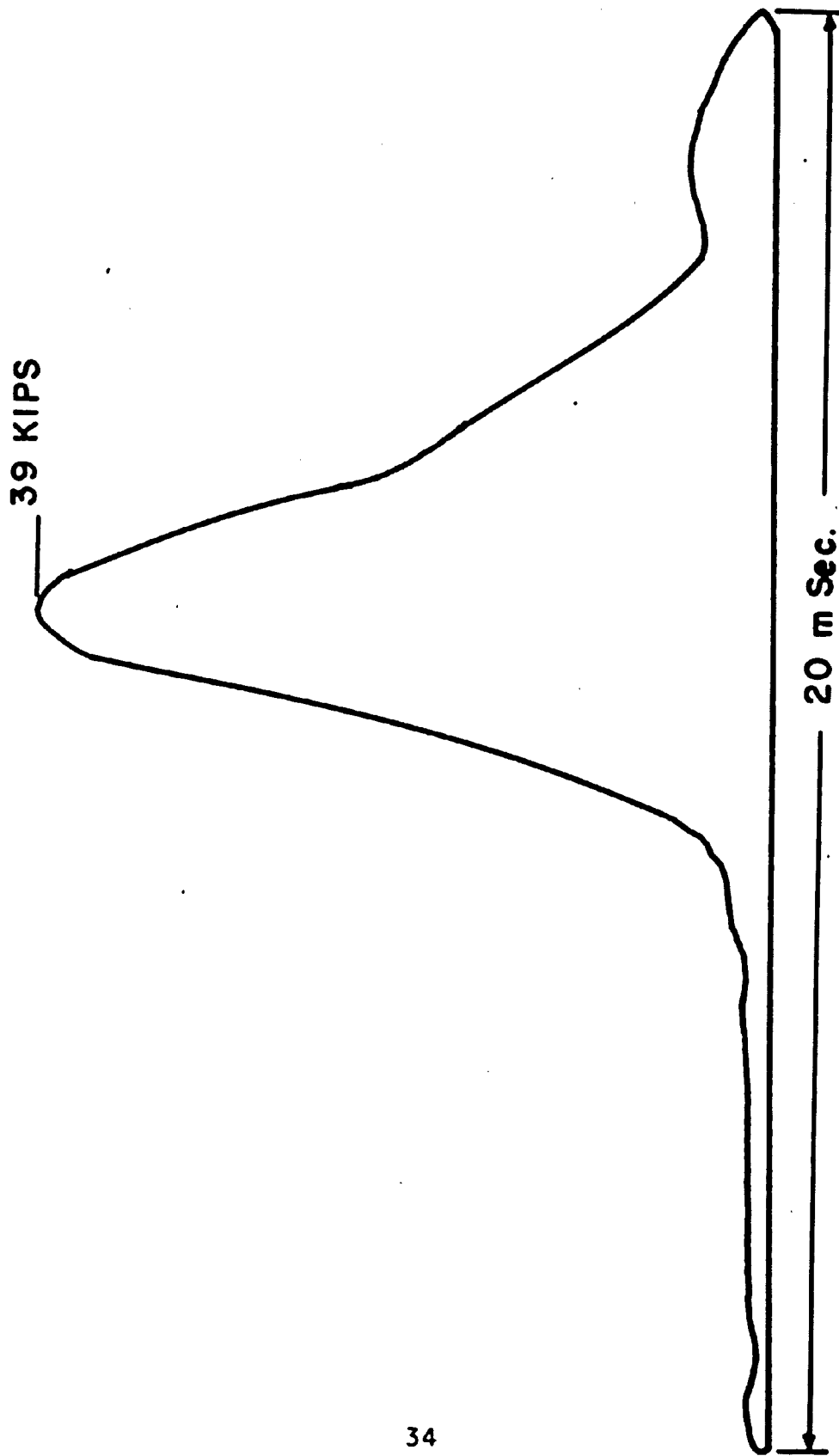


Fig.1 2-inch Thickness Compact Specimen



**Fig.2 Time VS Load Trace of Dynamic Loading**

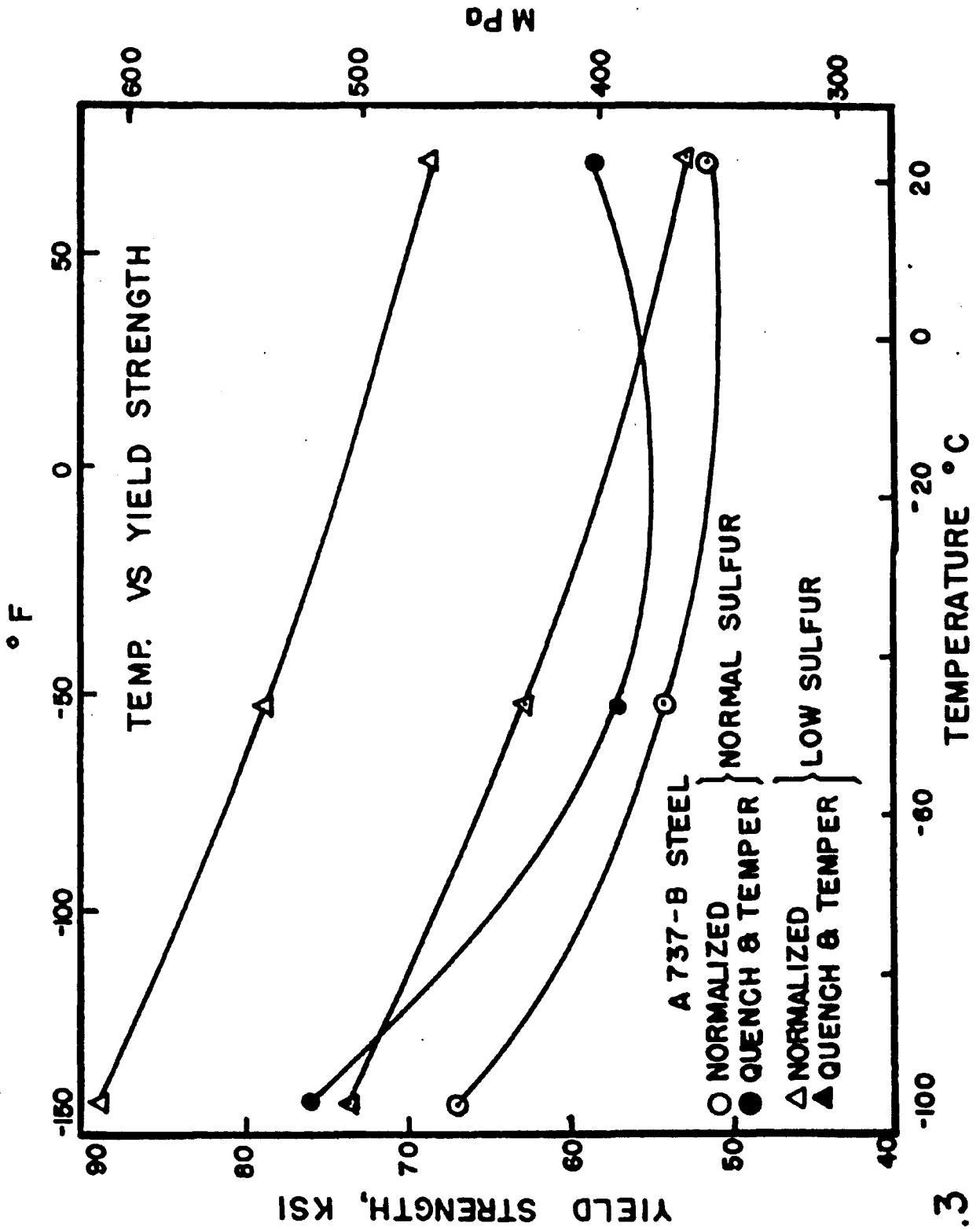


Fig.3

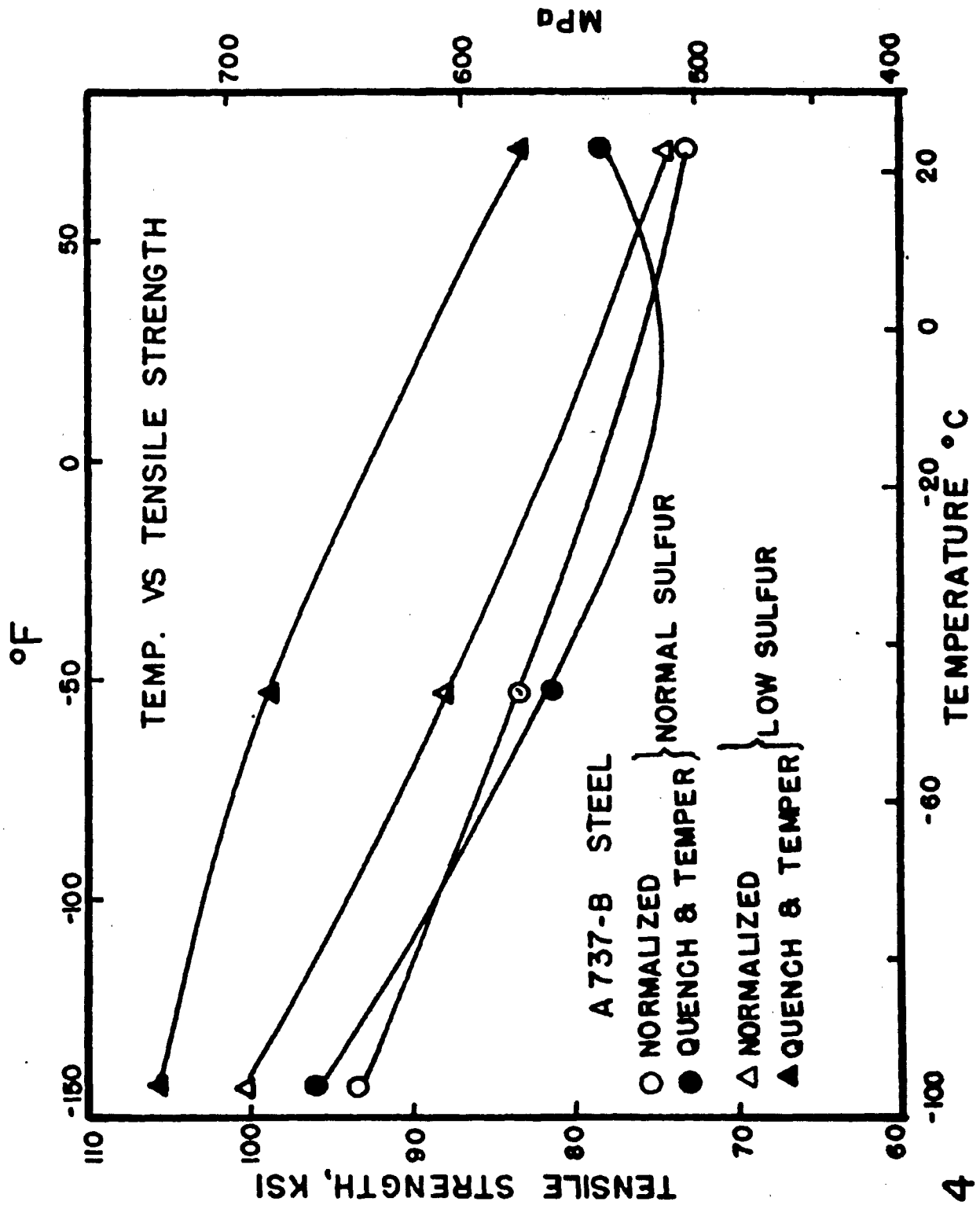


Fig. 4

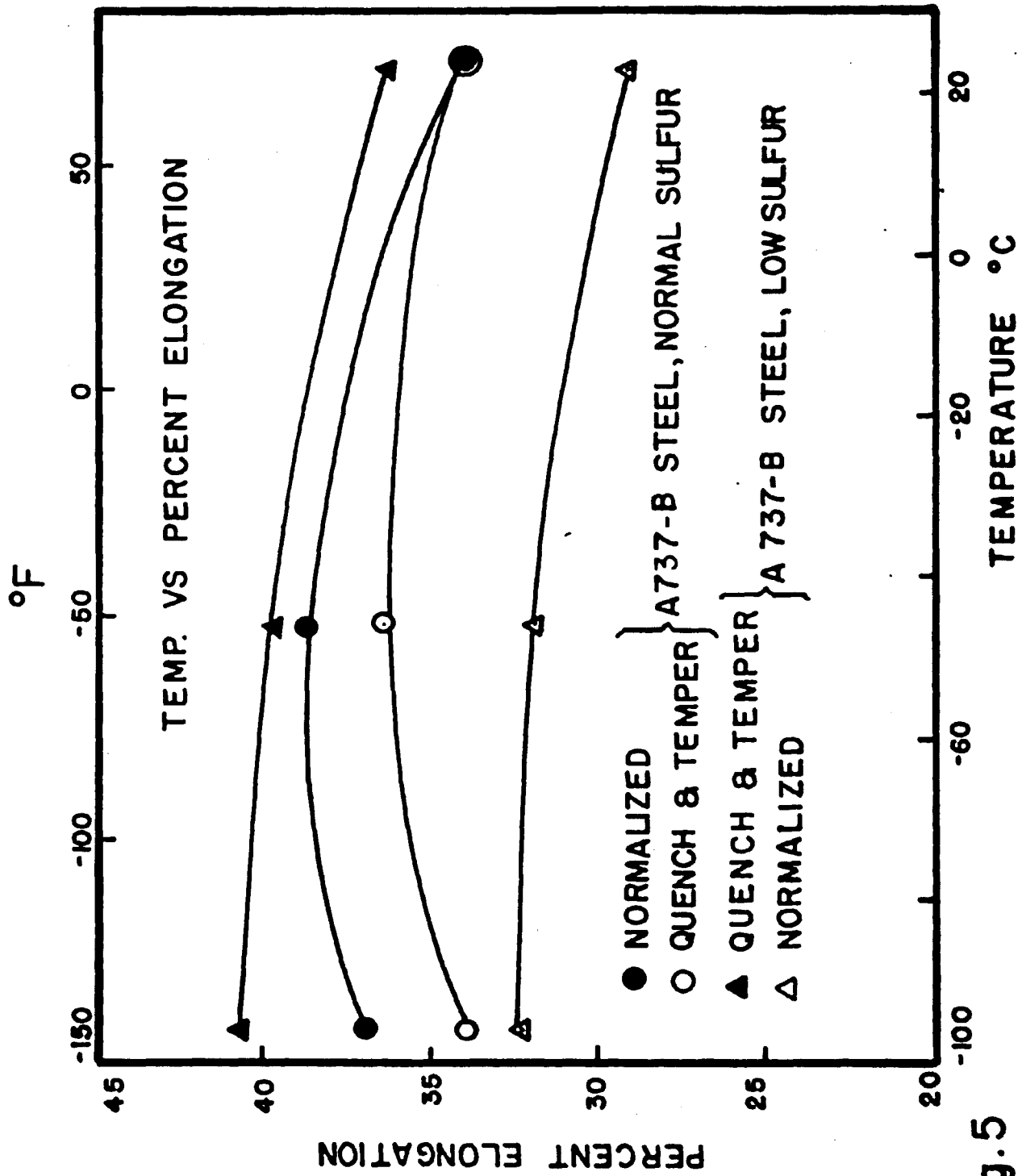


Fig. 5

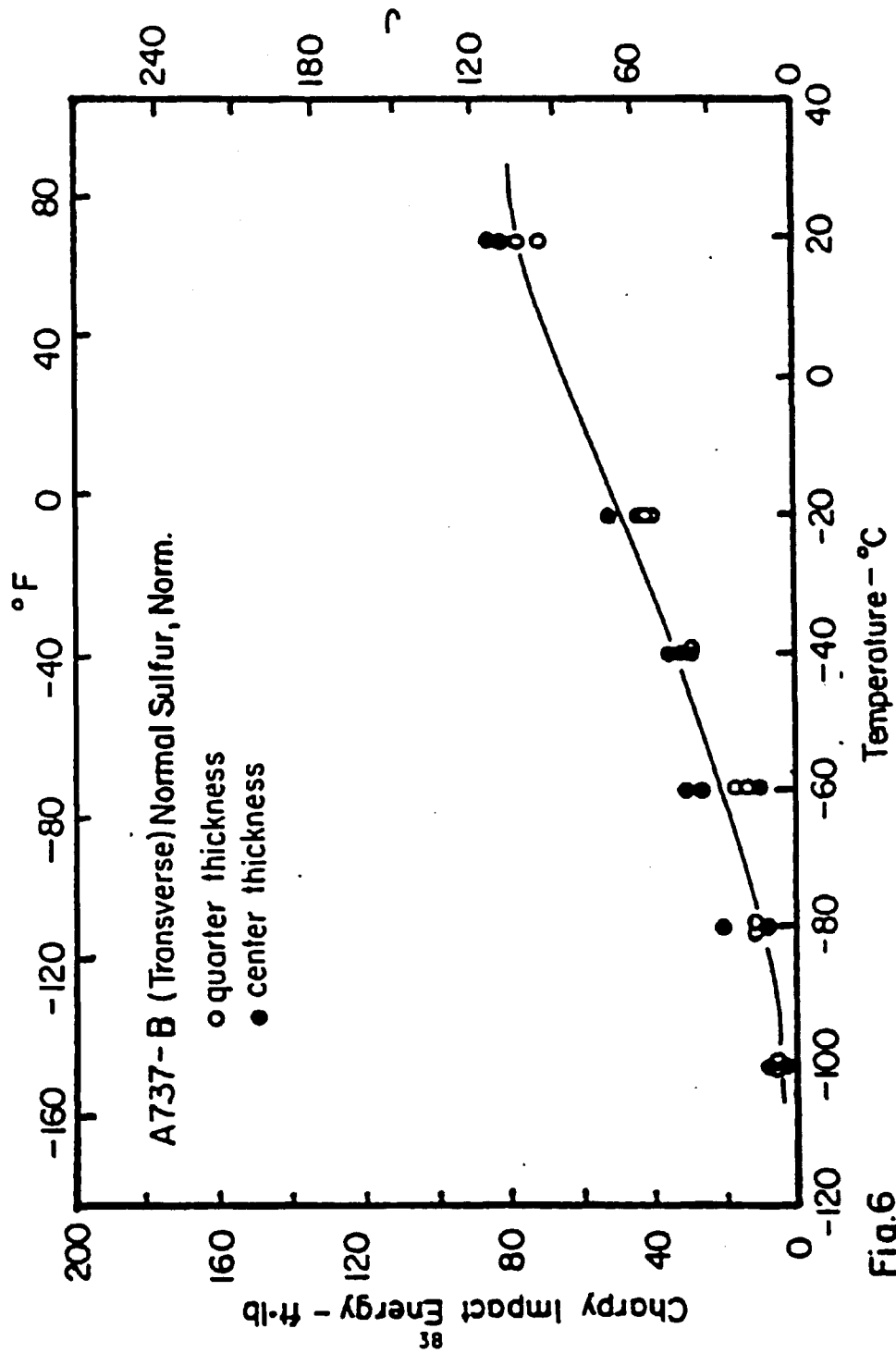


Fig.6



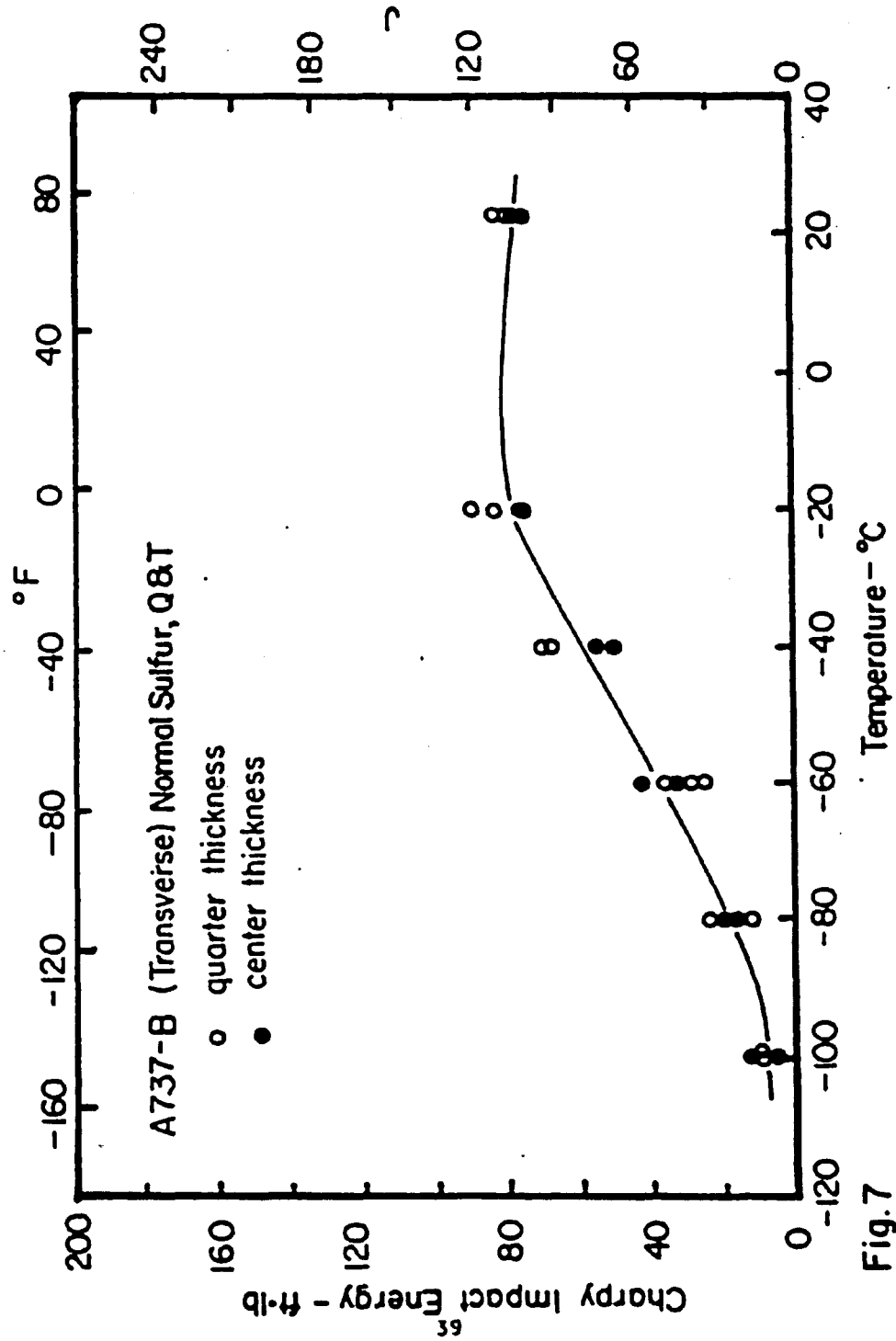


Fig. 7

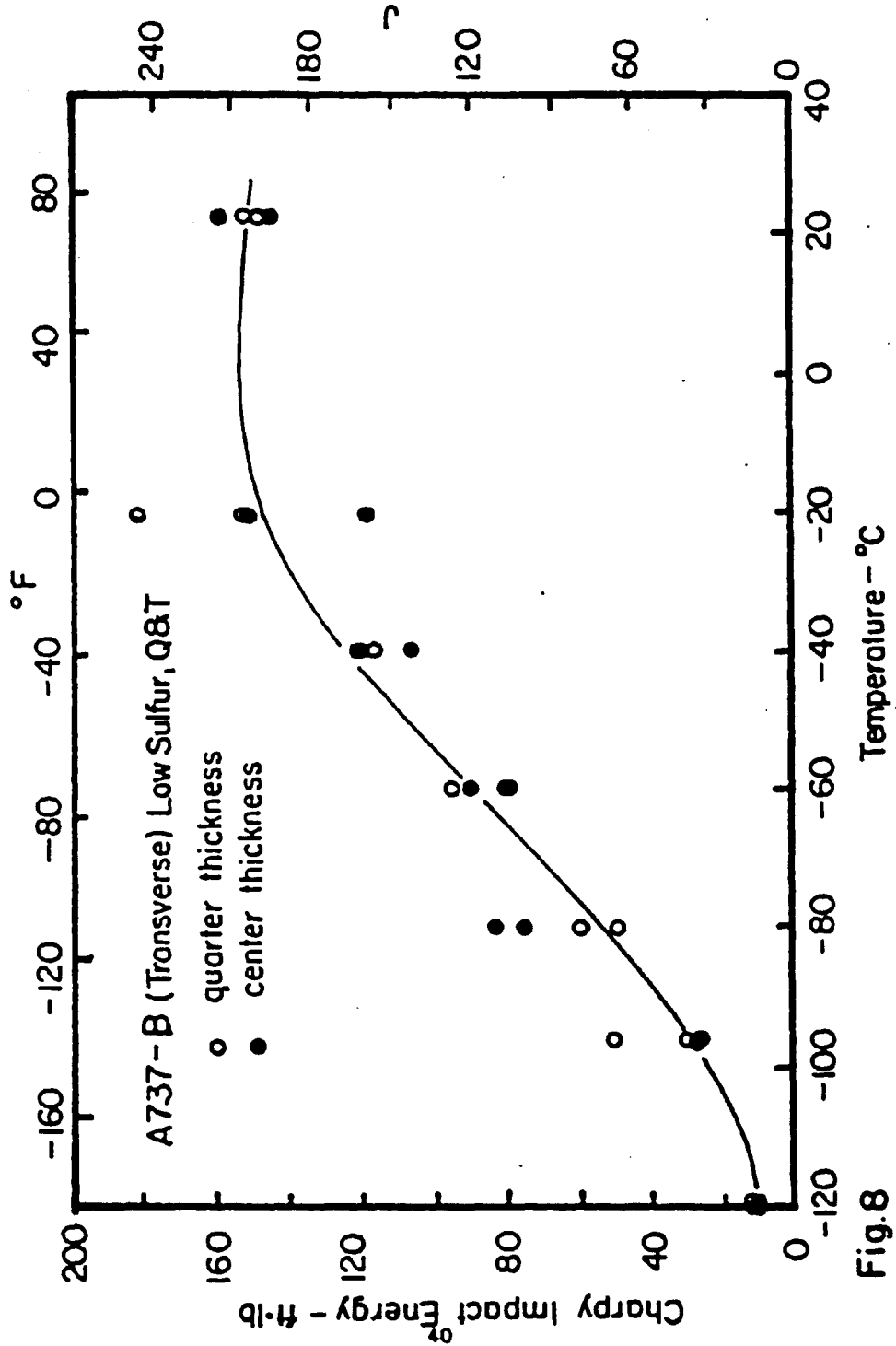


Fig.8

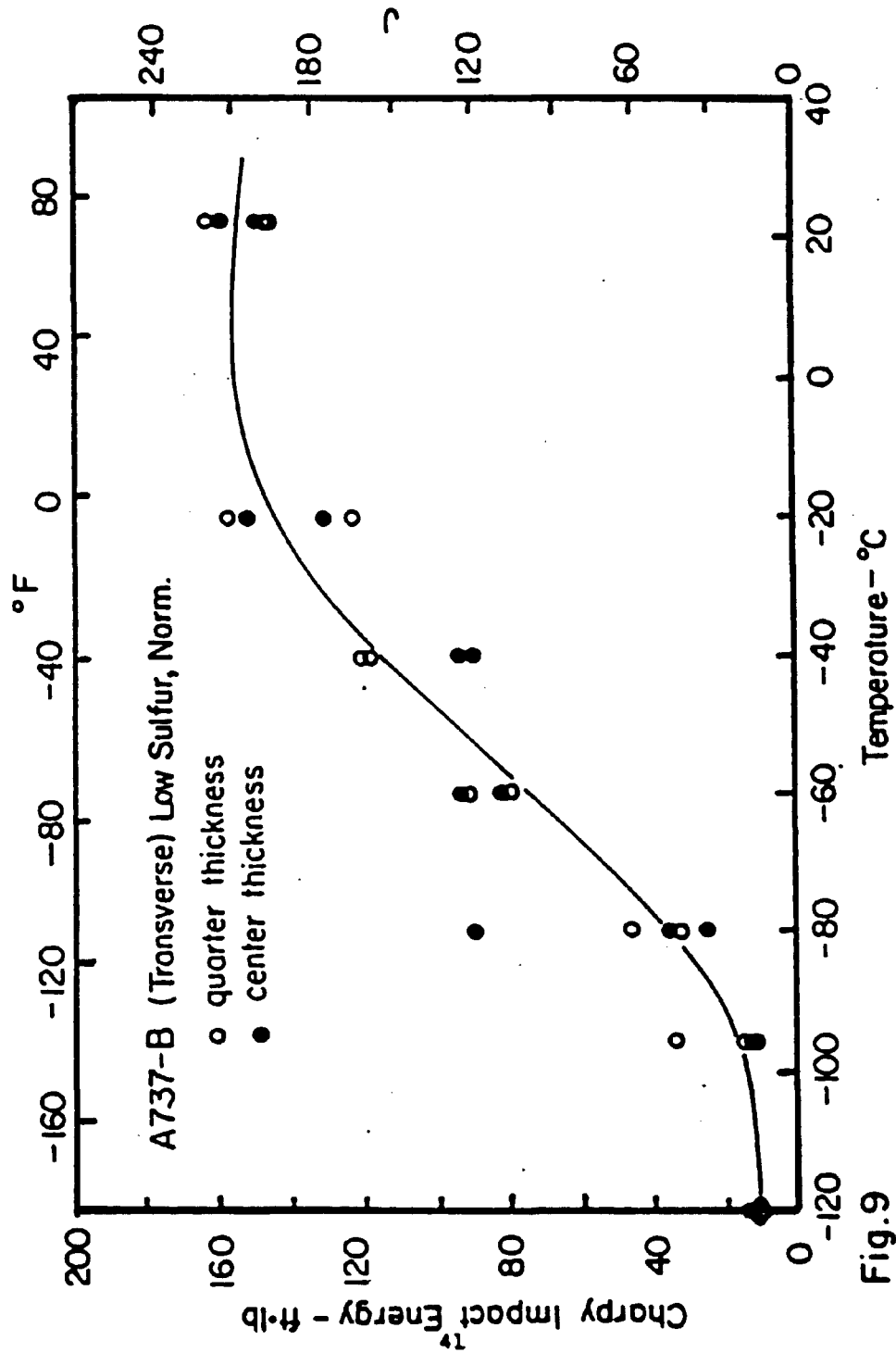


Fig.9

QUENCHED AND TEMPERED

NORMALIZED



Fig. 10 A-100X

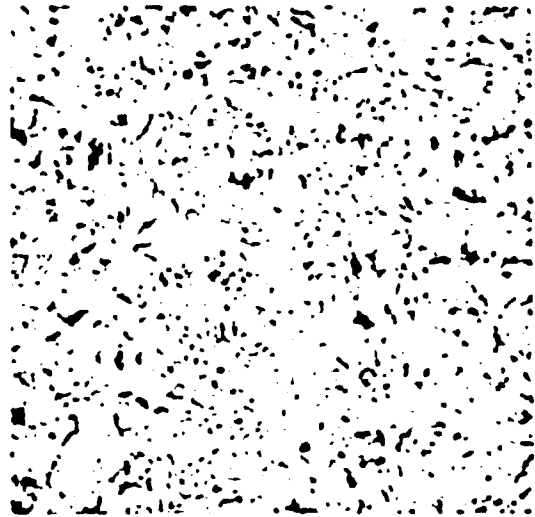


Fig. 10 C-100X

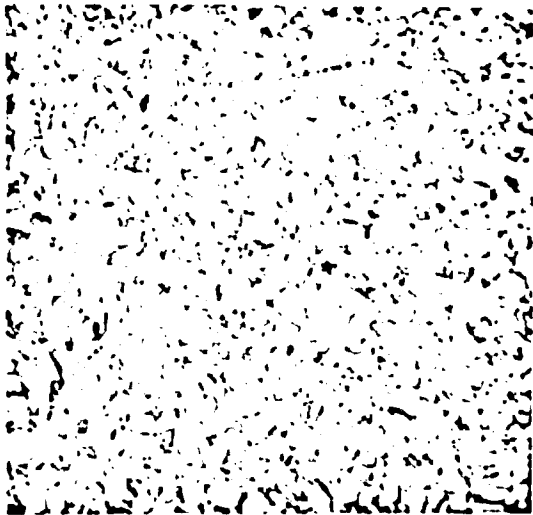


Fig. 10 B-500X

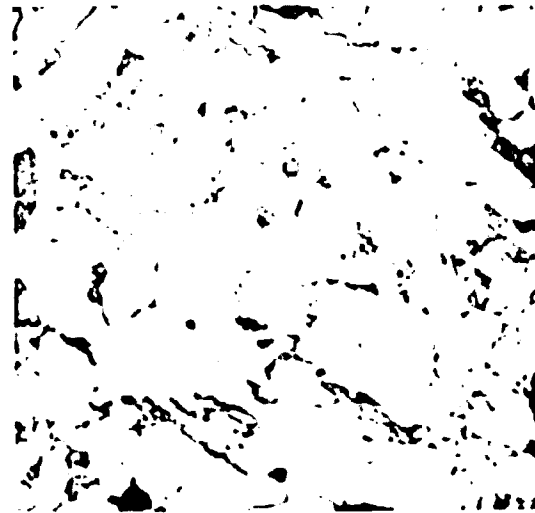


Fig. 10 D-500X

2% Nital Etch

Figure 10 Microstructure of the Normal Sulfur A737-B Steel

QUENCHED & TEMPERED

NORMALIZED

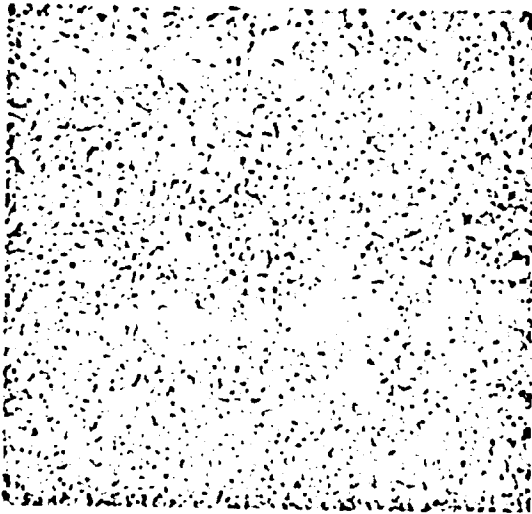


Fig. 11 A-100X

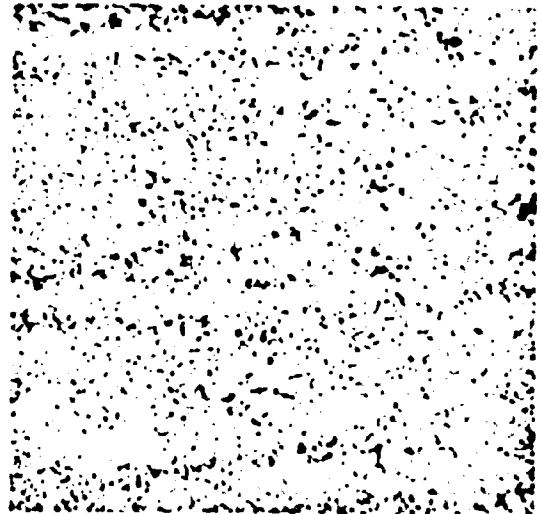


Fig. 11 C-100X

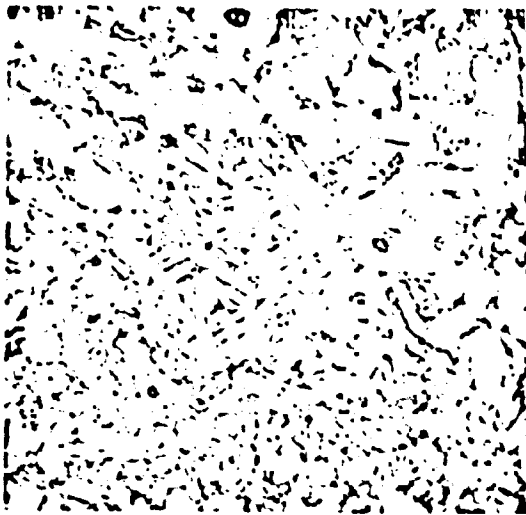


Fig. 11 B-500X

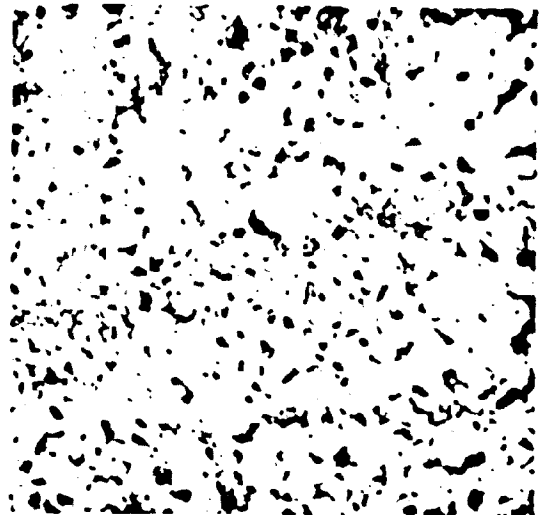


Fig. 11 D-500X

2% Nital Etch

Figure 11 Microstructure of the Low Sulfur A737-B Steel

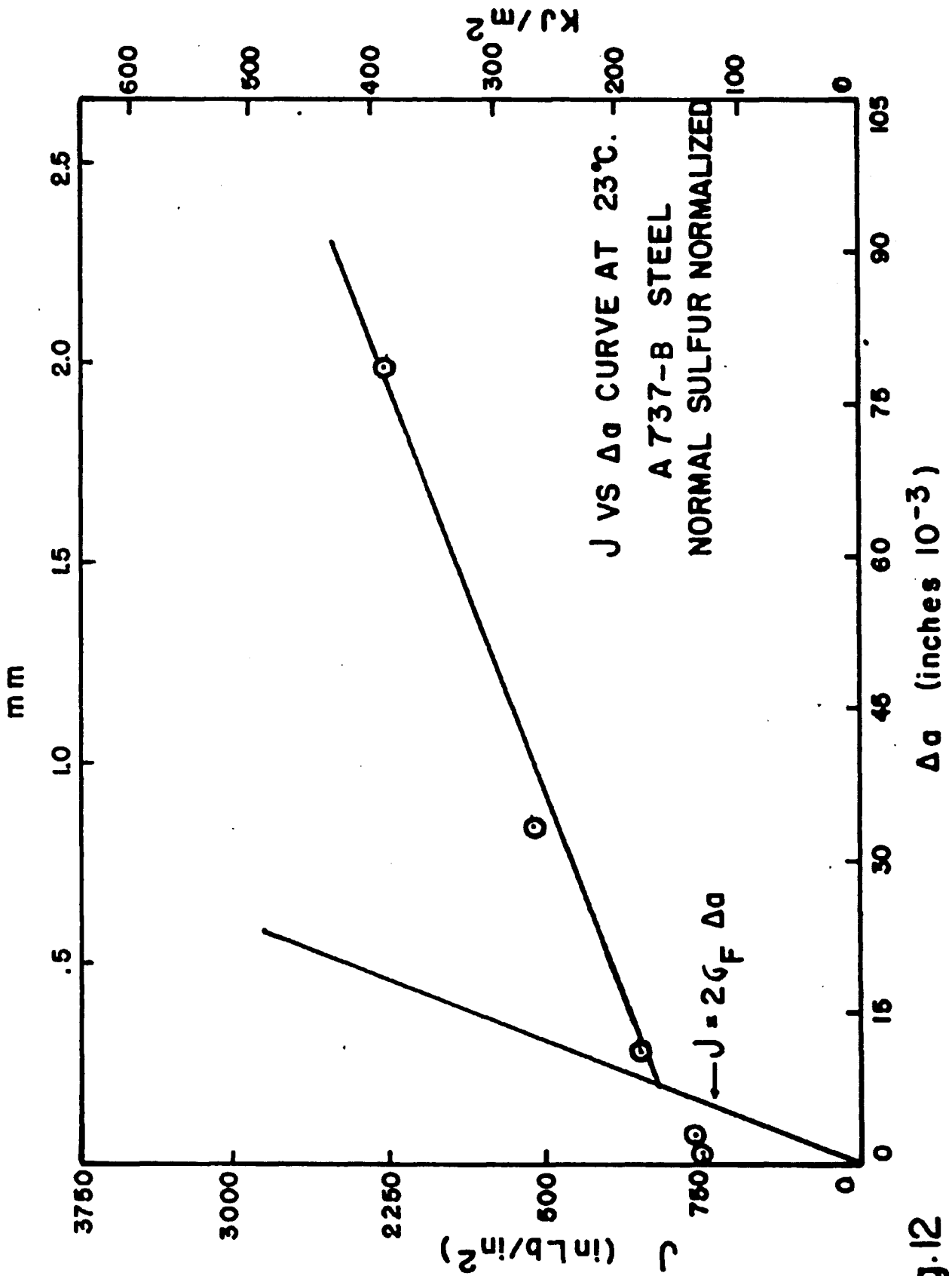


Fig.12

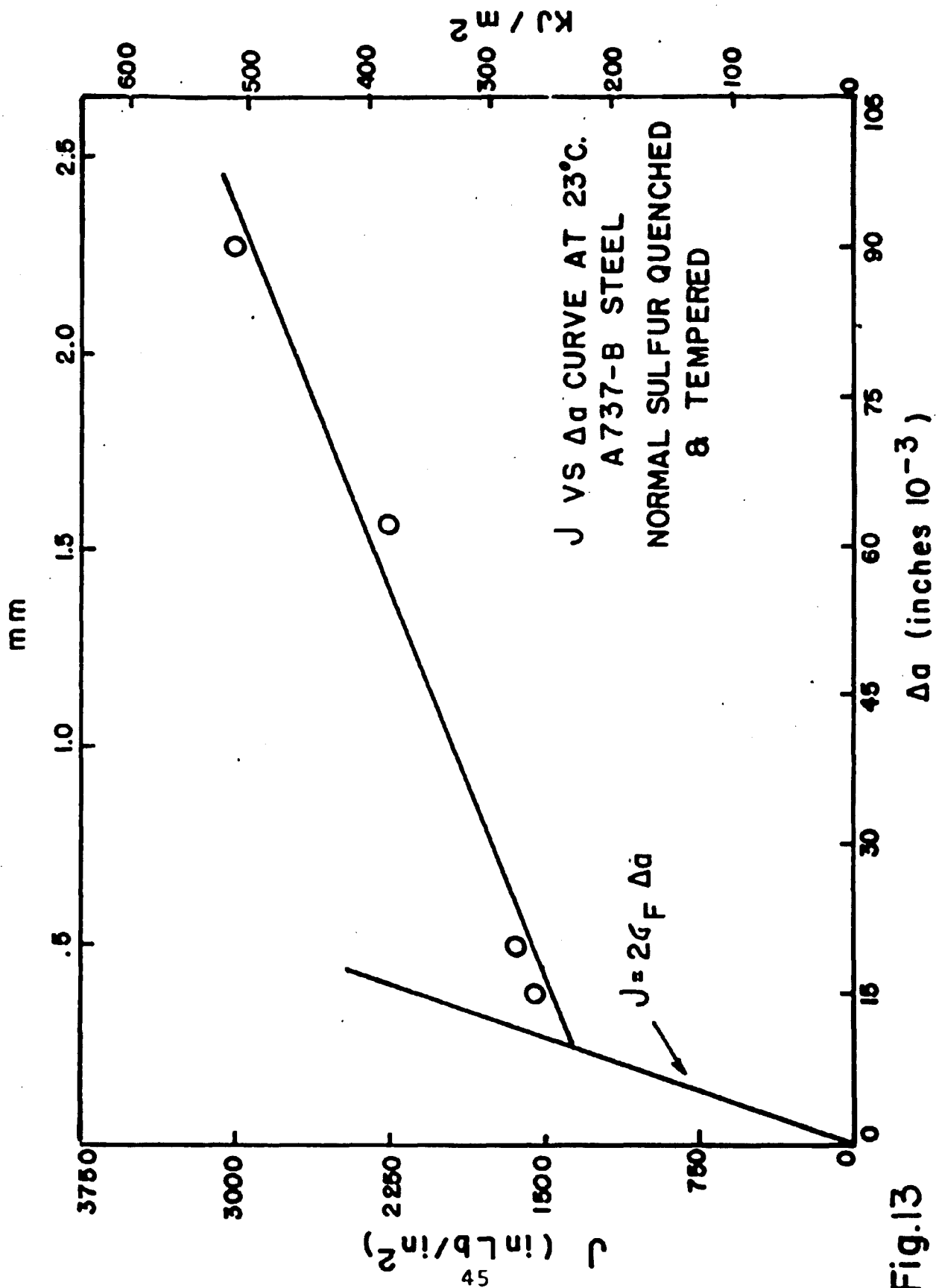


Fig.13

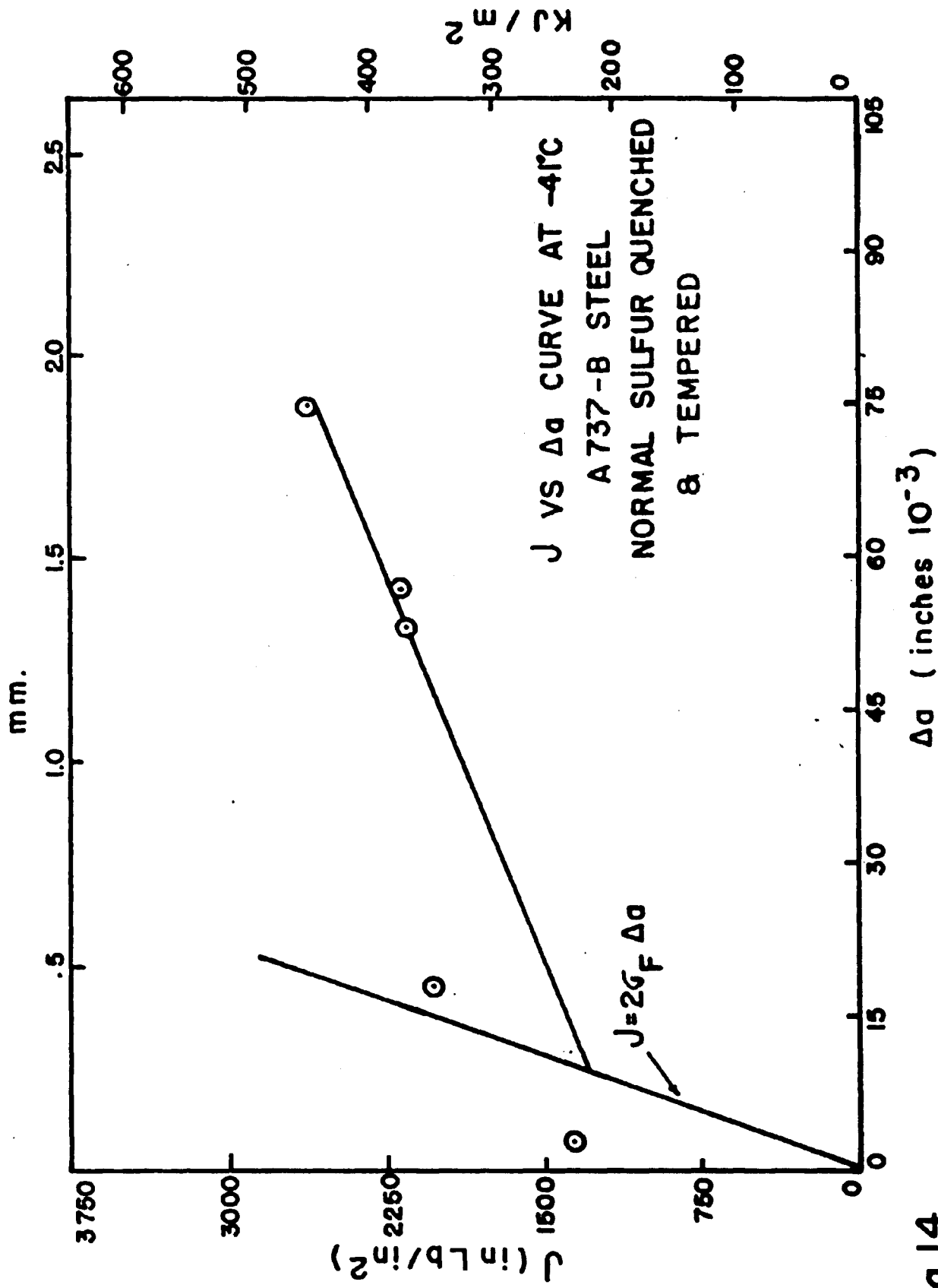


Fig. 14



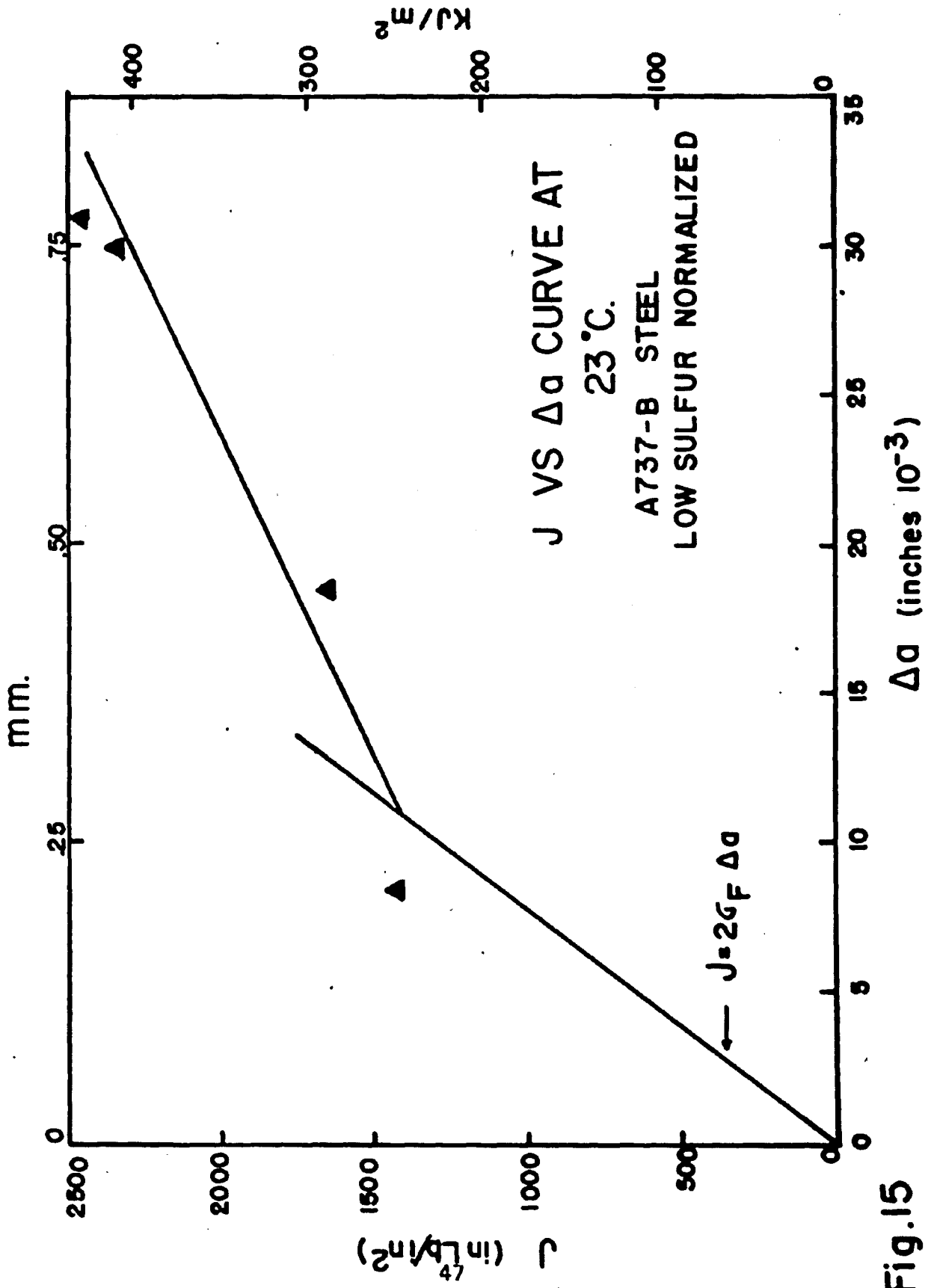


Fig.15

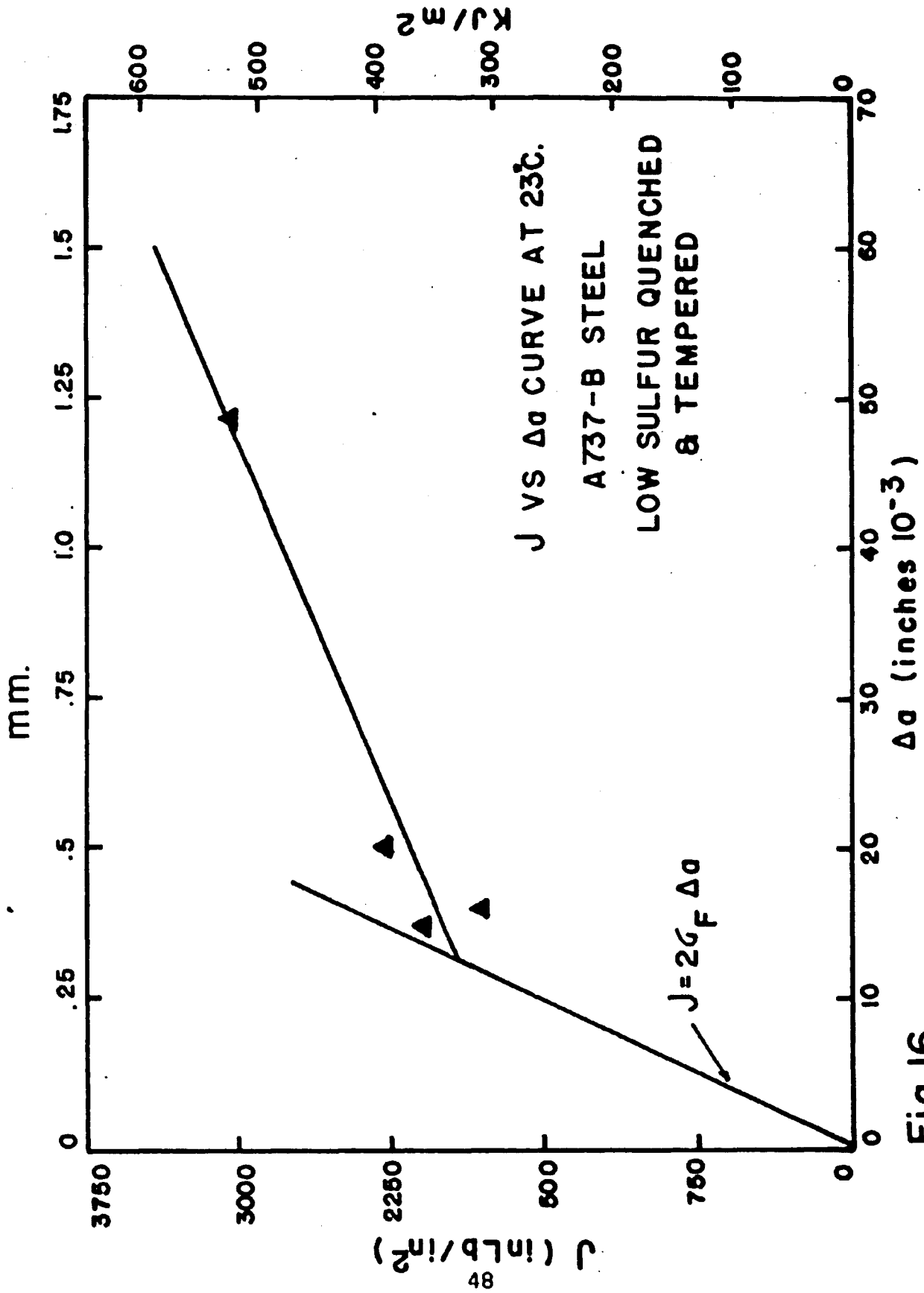


Fig.16

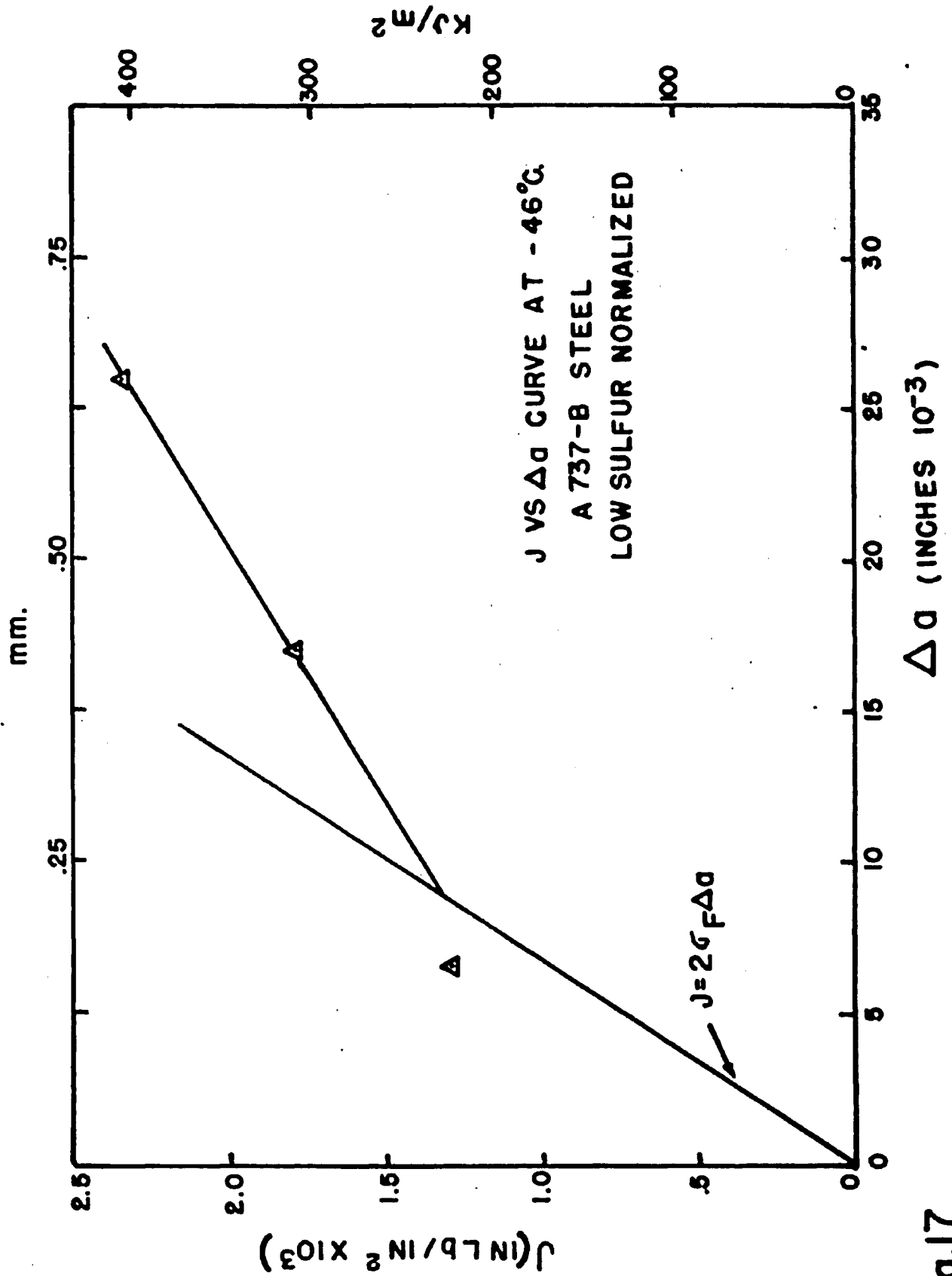


Fig.17

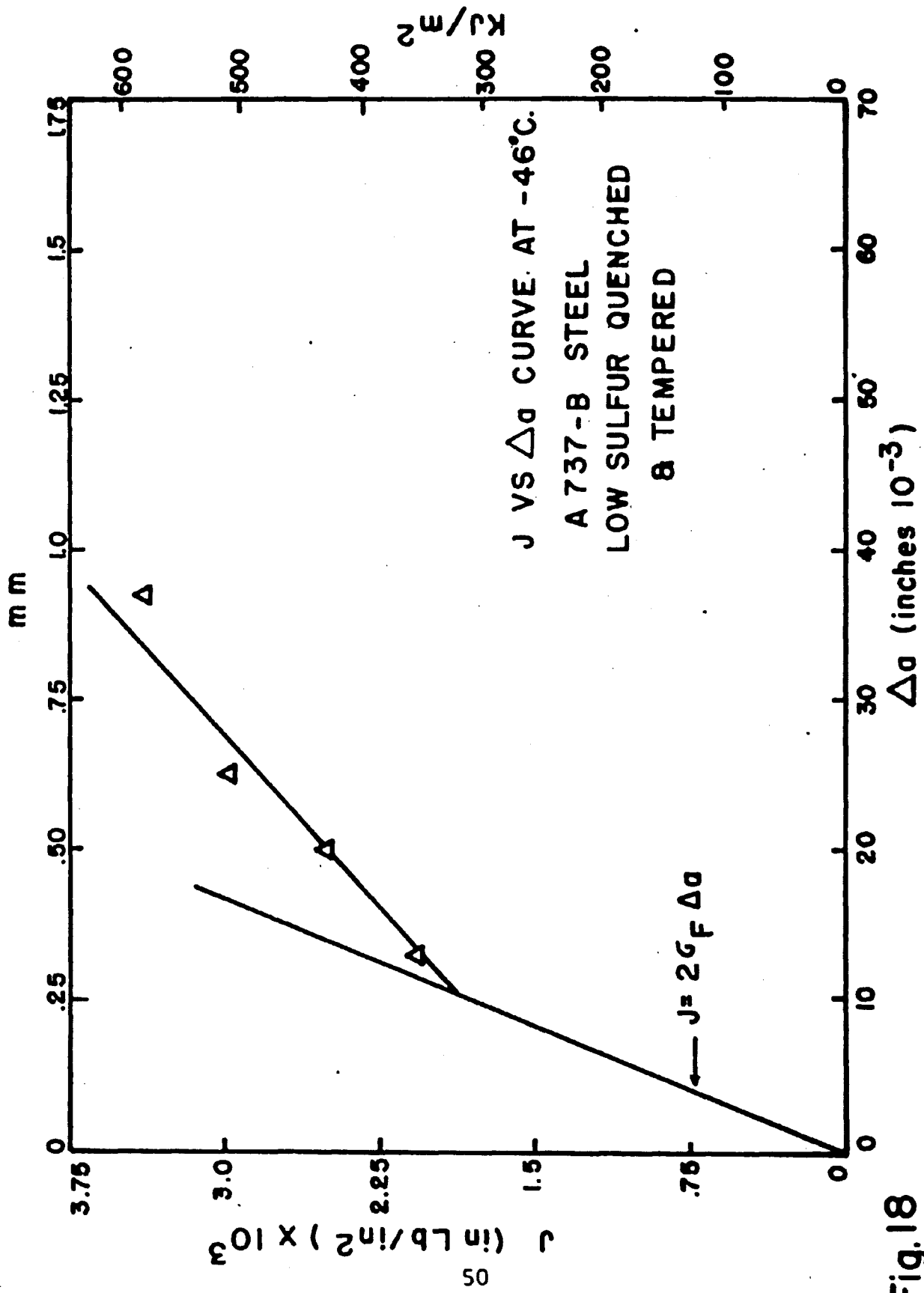


Fig. 18

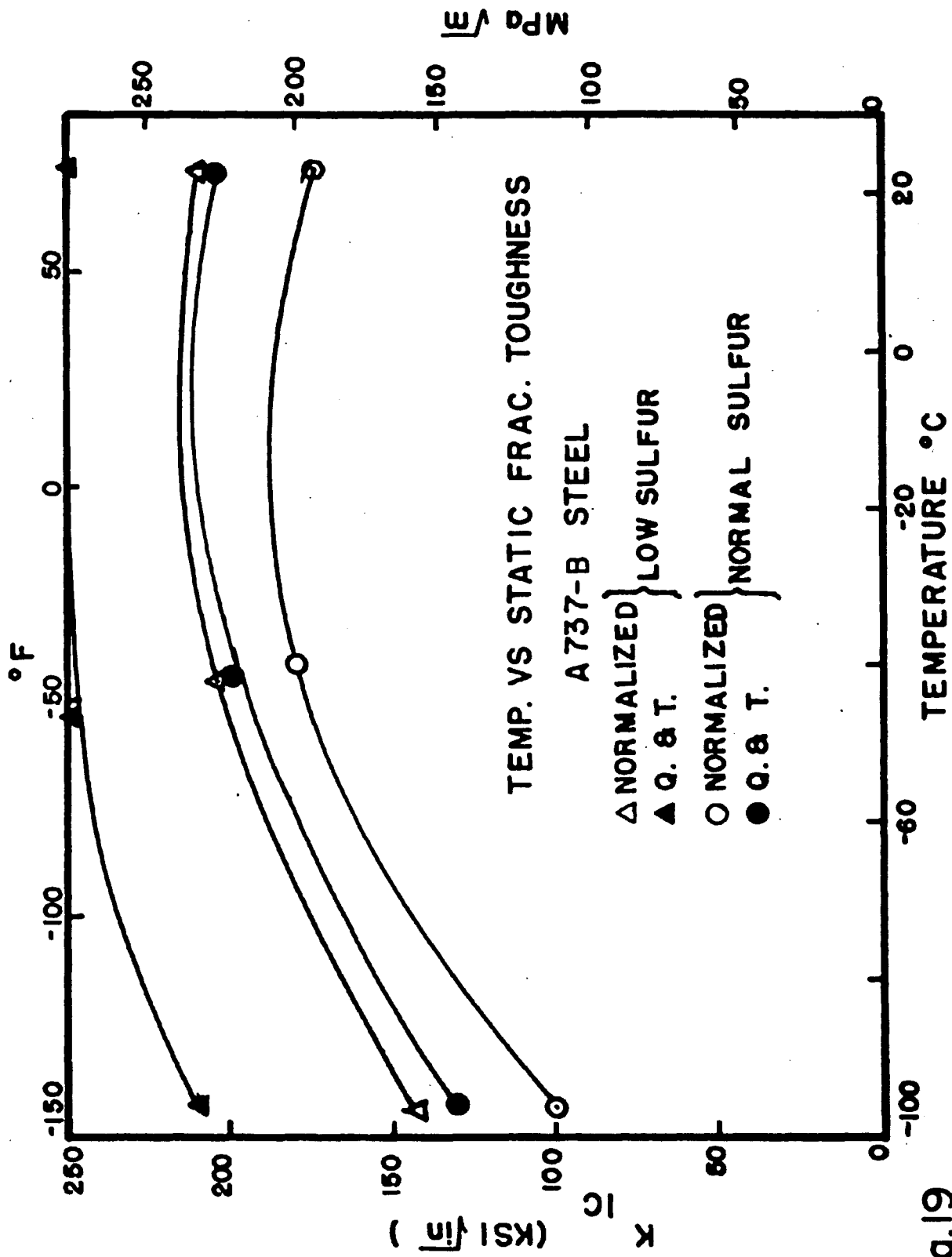


Fig. 19

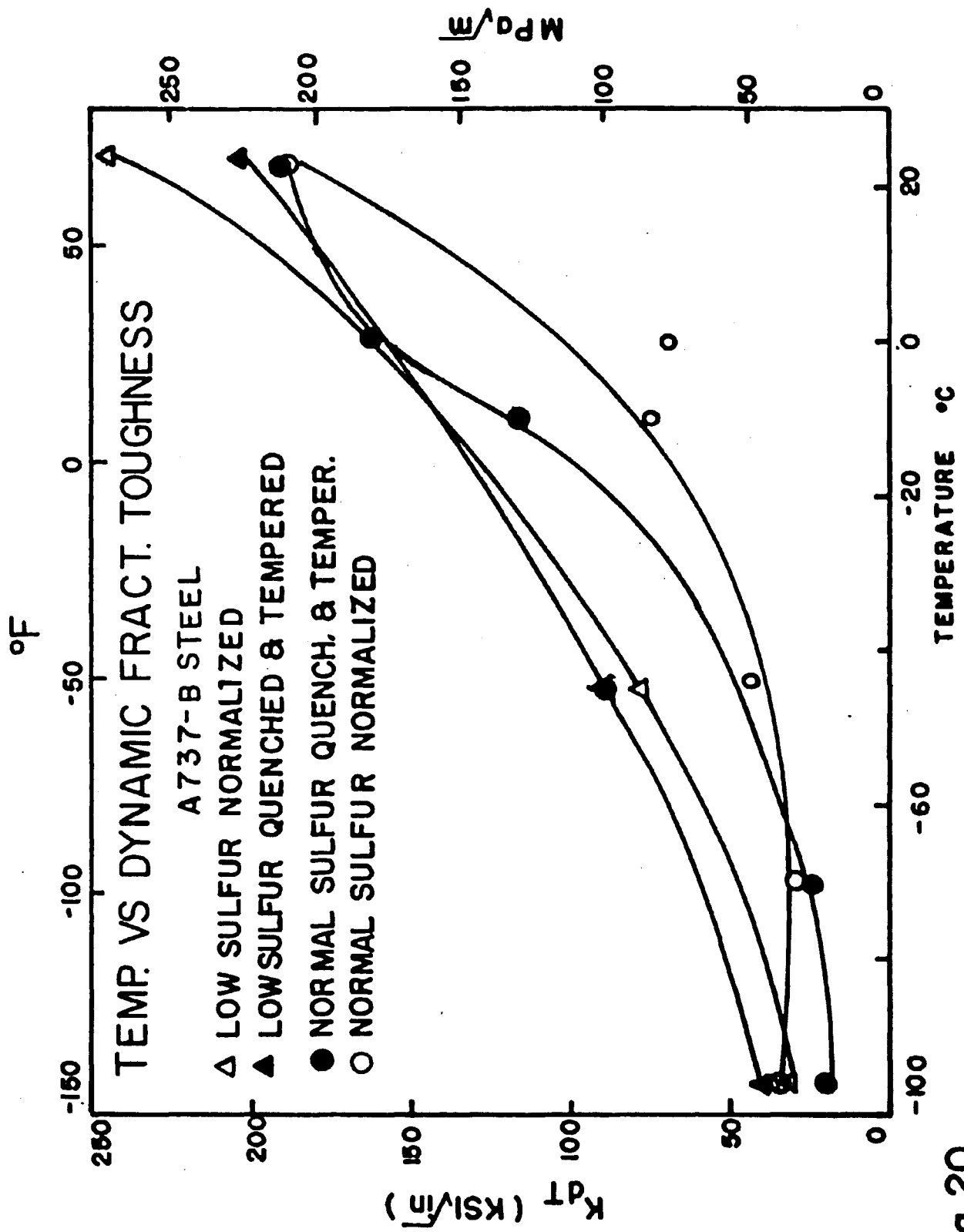


Fig. 20

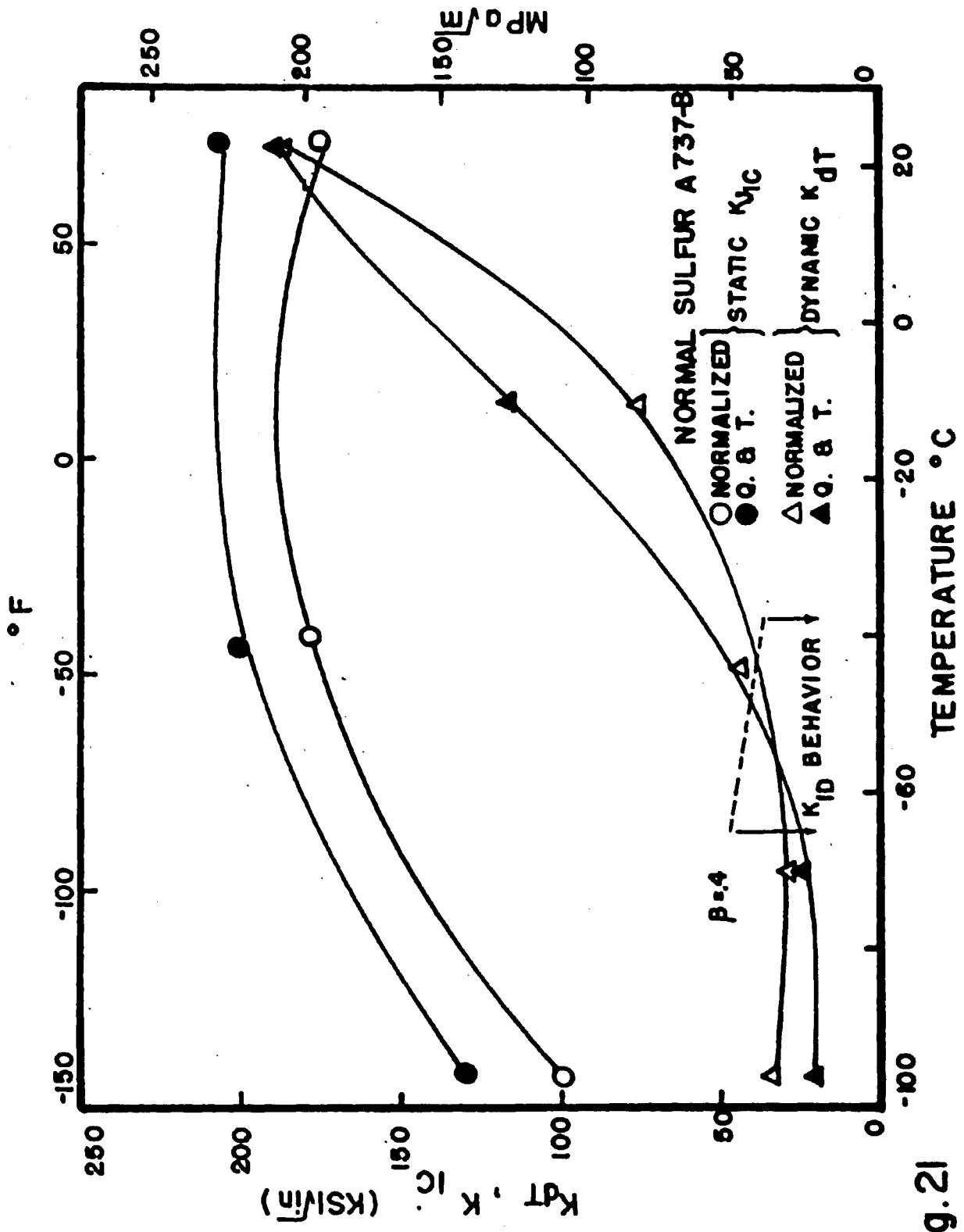


Fig. 21

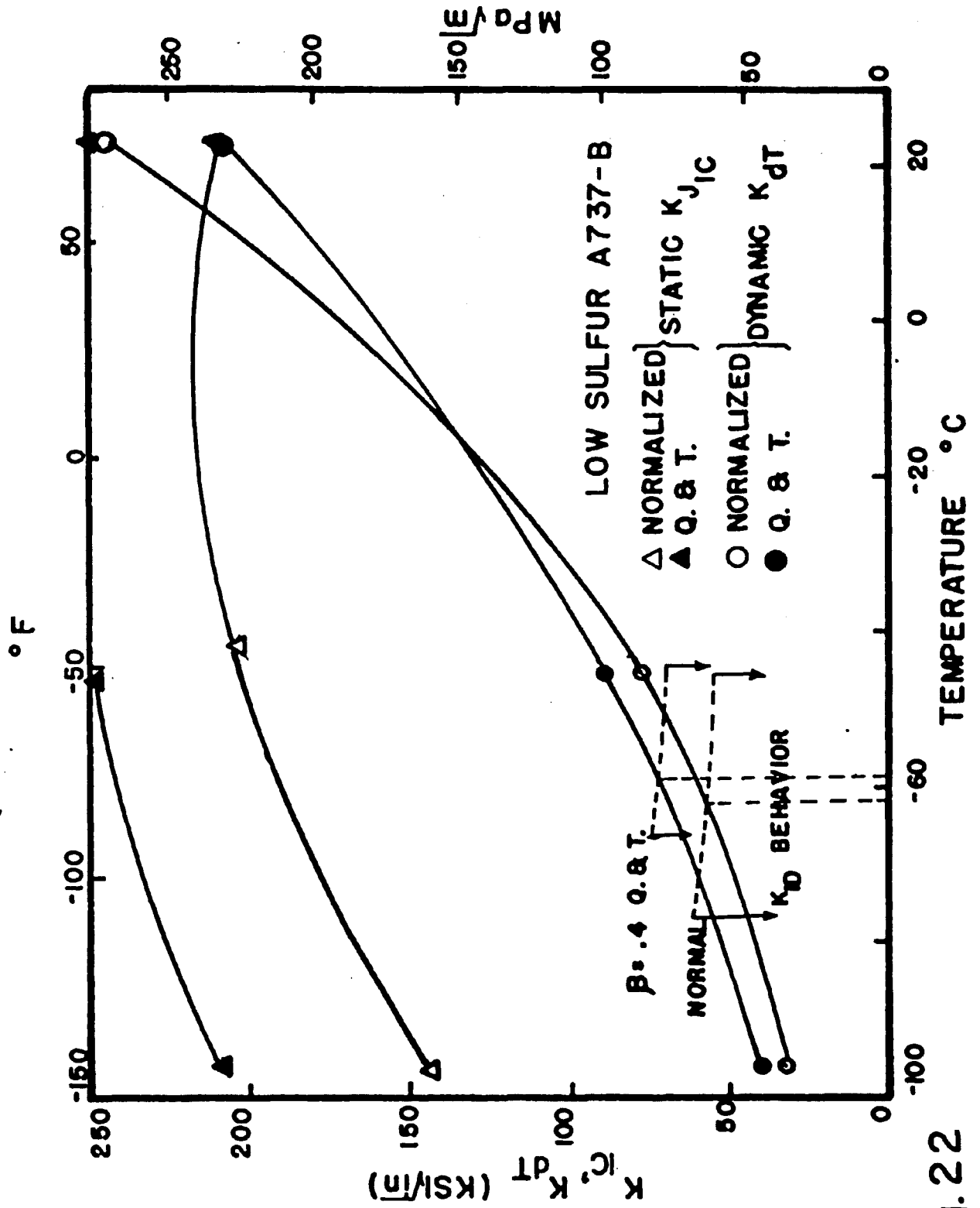


Fig. 22



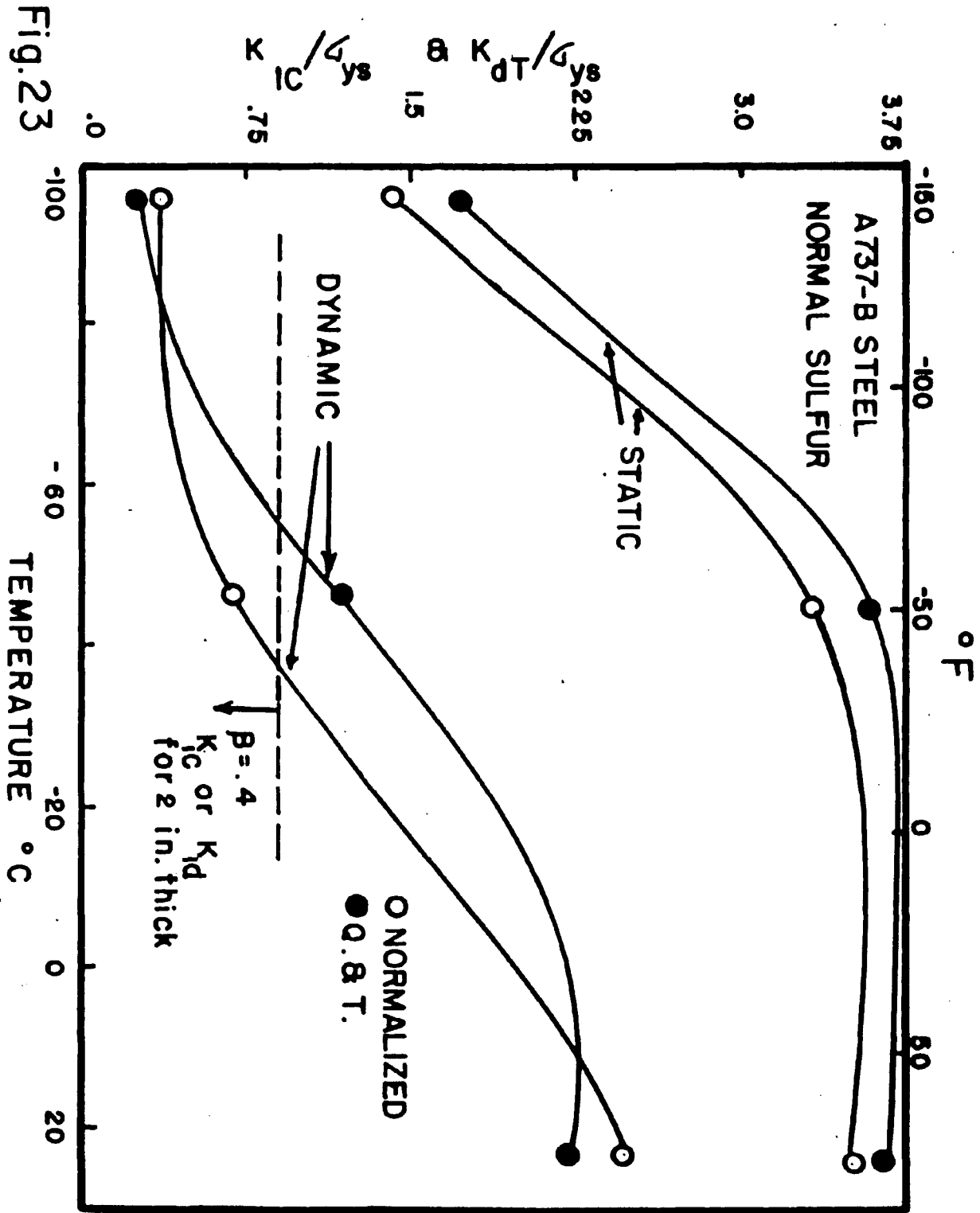


Fig. 23

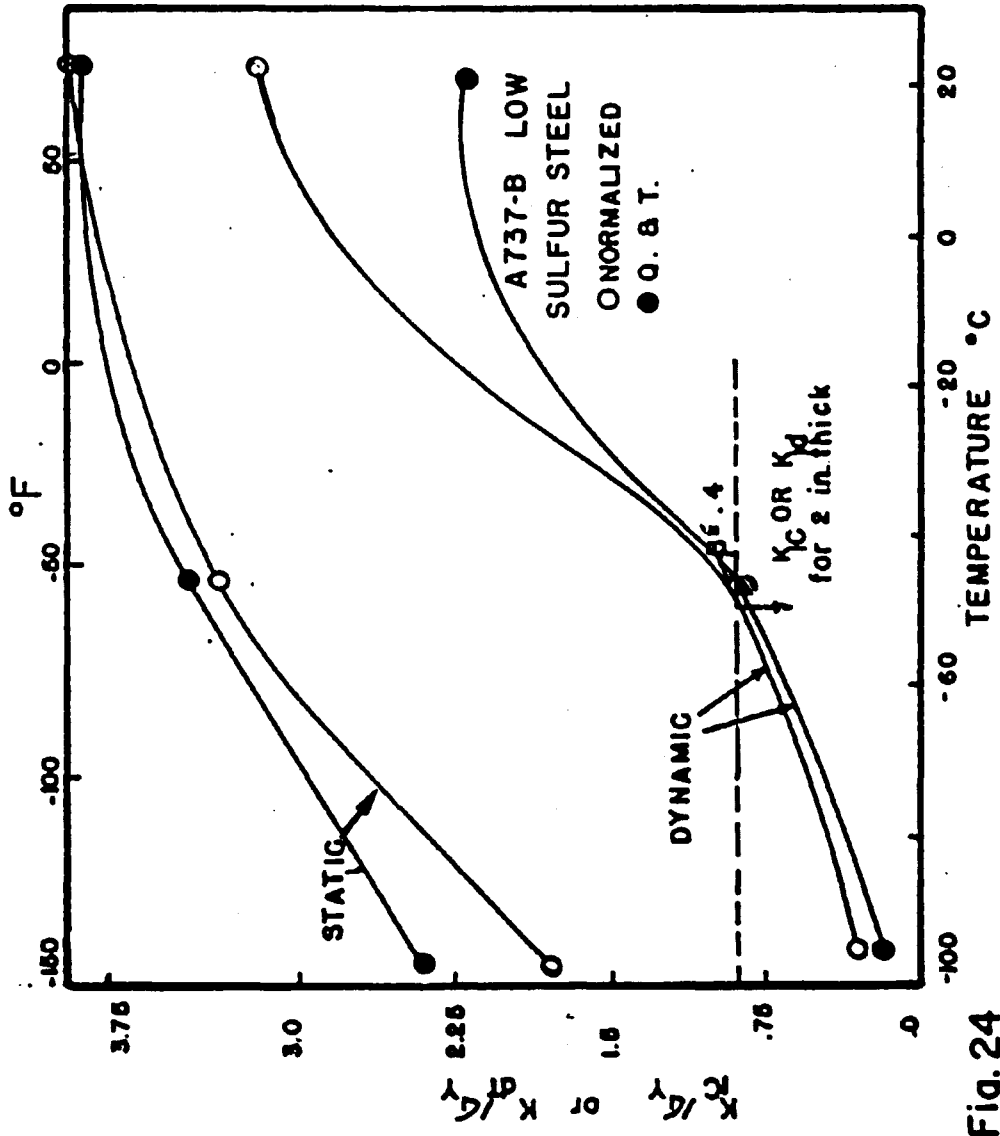


Fig. 24

## REFERENCES

1. E. H. Gillespie, "The Fracture Toughness of High Strength Nuclear Reactor Materials," March 26, 1976, Master's Thesis, Department of Metallurgy and Materials Science, Lehigh University
2. L. P. Trozzo, "A Fracture Toughness Analysis of A533 Grade B Plate For Pressure Vessel Service," April 1978, Master's Thesis, Department of Metallurgy and Materials Engineering, Lehigh Univ.
3. J. R. Rice, P. C. Paris and J. G. Merkle, "Some Further Results of J-Integral Analysis and Estimates," Progress in Flaw Growth and Fracture Toughness Testing, ASTM STP 536, American Society for Testing and Materials, 1973, pp. 231-245.
4. J. G. Merkle and H. T. Corten, "A J-Integral Analysis for the Compact Specimen, Considering Axial Force as well as Bending Effects," ASME Paper No. 74-PVP-33, American Society of Mechanical Engineers, 1974.
5. J. D. Landes and J. A. Begley, "Test Results from J-Integral Studies: An Attempt to Establish a  $J_{Ic}$  Testing Procedure," Fracture Analysis, ASTM STP 560, American Society for Testing and Materials, 1974, pp. 170-186.
6. P.H.Francis, T. S. Crooke and A. Nagy, "The Effect of Strain Rate on the Toughness of Steel," Ship Structure Committee 275 (1978)
7. J. M. Barsom and S. M. Rolfe, "Correlations Between  $K_{Ic}$  and Charpy V-Notch Test Results in the Transition Temperature Range," Impact Testing of Metals, ASTM STP 466, 1970, pp.281-302.
8. A. K. Shoemaker and S. T. Rolfe, "The Static and Dynamic Low-Temperature Crack-Toughness Performance of Seven Structural Steels;" Engineering Fracture Mechanics, 1971, Vol. 2, pp.319-339.

VITA

JAVAID IQBAL QURESHI

Born: June 13, 1946 in Lahore, Pakistan to  
Surfraz and Abdul Hamid Qureshi

Education: B.Sc. Metallurgical Engineering in  
October 1969 from Pakistan University of  
Engineering Technology Lahore

Professional Experience:

Presently employed by Babcock & Wilcox,  
Lynchburg, Va.

Previous: six years experience in foundry.